Theor Chem Acc (2011) 130:279–297
DOI 10.1007/s00214-011-0975-z

REGULAR ARTICLE

Quantum chemical studies on the role of water microsolvation in interactions between group 12 metal species (Hg^{2+}, Cd^{2+}, and Zn^{2+}) and neutral and deprotonated cysteines

Seiji Mori · Takahiro Endoh · Yuki Yaguchi · Yuuhei Shimizu · Takayoshi Kishi · Tetsuya K. Yanai

Received: 4 February 2011 / Accepted: 8 June 2011 / Published online: 23 June 2011

Abstract Interactions of group 12 metal(II) species (Hg^{2+}, Cd^{2+}, Zn^{2+}, $Hg(H_2O)_n^{2+}$, $Cd(H_2O)_n^{2+}$, and $Zn(H_2O)_n^{2+}$ ($n = 1, 2$) with neutral (RSH), deprotonated (RS^-), and doubly deprotonated cysteine species (abbreviated as "H_2cys", "$Hcys^-$", and "cys^{2-}", respectively) are examined with the Becke three-parameter Lee–Yang–Parr (B3LYP) hybrid functional after preliminary screening in a conformation analysis with the Parameterized Model number 3 (PM3) semiempirical method. Effects of water on aqueous solution are evaluated by microsolvation and polarized continuum model (PCM) approaches. In the most stable conformations of $M(H_2cys)^{2+}$ and $M(Hcys)^+$ complexes ($M = Hg^{2+}$, Cd^{2+}, and Zn^{2+}), the SH group of the cysteine moiety is already deprotonated and undergoes strong binding with the metal ion. Among $Hg(H_2cys)^{2+}$ complexes, cysteine complexes of Hg^{2+} without deprotonation of the SH group and mercury(II) carboxylato-type structures are at least 83 and 117 kJ/mol less stable in energy than the most stable complex (B3LYP/6-311++G(d,p)-SDD+d+f//B3LYP/6-31G(d)-SDD+d). Although Zn^{2+} binds more strongly than Hg^{2+} to a H_2cys molecule at the high-level CCSD(T)/6-311++G(d,p)-SDD+d+f//B3LYP/6-311++G(d,p)-SDD+d+f level, $[Hg(H_2O)_2]^{2+}$ is stronger than $[Zn(H_2O)_2]^{2+}$ because the deformation of $[Zn(H_2O)_2]^{2+}$ required to bind to cys is much more than in $[Hg(H_2O)_2]^{2+}$. Complexes with a deprotonated cysteine, $M(Hcys)^+$ and M(cys), prefer a multidentate structure.

Keywords Mercury · Cadmium · Zinc · Cysteine · Molecular interaction · Density functional calculations

1 Introduction

Mercury and cadmium are two of important elements in the environment. Their roles in pollution and their effects on physiology have been studied for a long time [1–3]. Their ions can strongly bind to the SH groups of amino acids, peptides, and proteins recent example [4, 5]. Metalloenzymes, capable of binding many metal-cysteine residues, are also observed in cytochrome P450 [6–9] and metallothioneins [10–12]. Metallothioneins may be an active species in the chemical detoxification mechanisms. L-cysteine (H_2cys) is the only naturally occurring amino acid bearing a SH group and is a unique and an important residue of protein function. L-cysteine itself also plays a role in biochemical transformations and enhances the severity of the renal injury and the cell viability of neurons induced during mercury toxicity [13–18]. The initial rate of entry of intravenously injected $MeHg^+$ through the blood–brain barrier into the brain is enhanced by coadministration with L-cysteine [19]. X-ray diffraction, spectroscopic, and theoretical studies on cysteine structures have been reported [20–24]. Fernandez-Ramos et al. noted that PCM

Dedicated to Professor Shigeru Nagase on the occasion of his 65th birthday and published as part of the Nagase Festschrift Issue.

Electronic supplementary material The online version of this article (doi:10.1007/s00214-011-0975-z) contains supplementary material, which is available to authorized users.

S. Mori (✉) · T. Endoh · Y. Yaguchi · Y. Shimizu · T. Kishi · T. K. Yanai
Faculty of Science, Ibaraki University, Bunkyo, Mito 310-8512, Japan
e-mail: smori@mx.ibaraki.ac.jp

S. Mori
Frontier Research Center for Applied Atomic Sciences, Ibaraki University, Tokai, Ibaraki 319-1106, Japan

calculations predict a preference for the zwitterionic structures of cysteine in aqueous solution [22]. In X-ray structures of $HgCl_2(H_2cys)$, $HgCl(H_2cys)(Hcys)$, and MeHg(Hcys) complexes, for example, an SH group is generally deprotonated [25, 26]. Early ^1H and ^{13}C NMR studies showed that there are 1:1 and 1:2 complexes of Hg(II) salts and cysteine with the formation of an Hg-thiolate bond and that to some extent the oxygen of the COOH group may coordinate to the Hg atom in the 1:1 $Hg(H_2cys)^{2+}$ complex in acidic solution [27, 28]. Recent analyses by Electrospray Ionization (ESI) and tandem mass spectroscopies of mercury bis-thiolate in acidic solution also support the existence of $Hg(Hcys)(H_2cys)^+$ and its degradation products with Hg–S binding [29]. Earlier ^{13}C and ^1H NMR studies of mixtures of Hg(II) salts and cysteine at physiological pH indicate that Hg is strongly bound to two thiolate moieties in cysteine to form a linear-coordinated $Hg(cys)_2$ complex [30]. Recent Extend X-ray Absorption Fine Structure (EXAFS) and X-ray Absorption Near Edge Structure(XANES) studies in alkaline solution show the high stabilities of $Hg(cys)_2^{2-}$ and $Hg(cys)_3^{4-}$ with a strong Hg–S bond [31, 32]. The Hg–S moiety has also been found in cysteine-containing peptides and proteins since Hughes found an example in serum albumin with mercury(II) salts [33, 34]. Potentiometric titrations with the competing ligand diethylenetriaminepentaacetic acid for the formation constants of the 1:1 and 1:2 complexes of Hg(II) with glutathione (GSH) show the existence of the protonated GSH complexes with Hg(II) [35]. In NMR studies of metal complexation with a glutathione, Cd^{2+} and Zn^{2+} groups bind to both the SH and glutamyl NH_2 groups, while Hg^{2+} binds to only the SH group [36]. The recent Hg L_{III}-edge EXAFS studies for Hg(II)-GSH complexes in neutral aqueous solution supported the Hg–S bonding [37]. There are cases for interaction between mercury and cysteine residues in organomercurial lyase MerB and ethylmercury(II) labeled protein [5, 38].

Cadmium ion toxicity also exhibits the substitution of a calcium ion in tissues such as kidney, lungs, bone, and muscle because of the similar sizes of cadmium and calcium ions. Simultaneous coexposure to low doses of inorganic mercury and cadmium results in an overall decrease in the renal burden of mercury and an increased rate in the urinary excretion of mercury [39]. The Cd(II) ion can substitute Zn(II)-containing enzymes and proteins to affect the homeostasis and signaling events [1, 40]. Speciation for Cd(II)-cysteine complexes in aqueous solution with an NaCl medium was performed at a range of $4 < pH < 8$ [41]. The spectroscopic studies of solid $\{Cd(Hcys)_2{\cdot}H_2O\}_2{\cdot}H_3O^+ClO_4^-$ and $Cd(Hcys)_2{\cdot}H_2O$ indicate a deprotonated thiolate ion coordination into the Cd(II) ion and no coordination of $-NH_3^+$ group into the Cd(II) ion [42]. The CdS nanoparticle that is used as semiconductor is also prepared using cadmium(II) salts and cysteine [43, 44].

A zinc(II) ion, which belongs to the same elemental group as mercury(II) and cadmium(II) ions and is one of the most important metals in human body, not only binds to a thiolate group (such as alcohol dehydrogenase) [45–47] but also to the carboxyl groups of biomolecules (such as glyoxalase I and carboxypeptidase A) [48, 49].

Binding of a metal ion with one cysteine molecule is one of the most fundamental interactions in biological chemistry and toxicology [50]. After the seminal paper on the mass spectroscopy [51], theoretical studies on $Cu^I(H_2cys)^+$ were performed by Ohanessian and coworkers [52]. Density Functional Theory (DFT) studies on the structures of $[Pt(NH_3)_2Cl(H_2cys)]^+$, $Co(H_2cys)^{2+}$, and $Co(Hcys)^{2+}$ have been reported recently [53, 54]. The structures of conformers for $Hg(H_2cys)^{2+}$, $Cd(H_2cys)^{2+}$, $Zn(H_2cys)^{2+}$, and $Cu^{II}(H_2cys)^{2+}$ have already been reported by the groups of Russo and others with the aid of Becke three-parameter Lee–Yang–Parr (B3LYP) hybrid functional with basis sets of LANL2DZ [55] for a metal and 6-311+G(d) for the other elements [56–59].[1] DFT calculations for Hg complexes including $Hg(SMe)_2$, MeHg(SMe), MeHg(Hcys), and $Hg(Hcys)_2$ were also performed [60–63]. They found that each metal ion showed different behavior in its binding of a cysteine molecule. According to the results reported by Russo et al., Zn^{2+} binds more strongly to cysteine than Hg^{2+} in the gas phase [56]. However, their works was based only on the five most stable conformers of the cysteine molecule. In addition, the Stuttgart-Dresden-Cologne effective core potential [64] was recently found to be a better description than LANL2DZ of the effective core potential for Hg bidentate complexes and $[M(OH_2)]^{2+}$ (M = Zn, Cd, and Hg) [65, 66]. From the formation constants [ML]/[M][L] and [MHL]/[M][HL] (M = Hg, Cd, and Zn, Table 1) in aqueous solution [67–73], the binding ability decreases in the following order: Hg(II) > Cd(II) ~ Zn(II). According to the stability constants of metal-cysteine complexes in aqueous solution, Hg^{2+}, Cd^{2+}, and Zn^{2+} are coordinated by more than two ligands [25, 27, 28].

Similar theoretical studies in the modeling of metal-cysteine complexes such as $ML_n(SMe)^{2+}$ (M = Co, Ni, Cu, Zn, Cd, Hg, L = H_2O, H_2S, im, NH_3), $Zn(im)_2(OH_2)(SMe)$, and $Zn(im)(OH_2)(SMe)_2$ were conducted [74–76]. In any of the previous studies, cysteine was modeled as HS^- and MeS^-. Theoretical studies on $Zn(His)_{4-n}(H_2cys)_n$ have also been reported [77]. Although there have been several reports published recently, the

[1] A part of the present studies are already orally communicated.

Table 1 Stability constants in the formation of metal-cysteine complexes

		$\log_{10}K$	Ionic strength (μ)	
Zn^{2+}	$\frac{[ML]}{[M][L]}$	9.11	25 °C	0.1
	$\frac{[ML_2]}{[M][L]^2}$	18.12	25 °C	0.1
		17.9	37 °C	0.15
	$\frac{[MHL]}{[M][HL]}$	4.60	25 °C	0.1
		4.54	37 °C	0.15
Cd^{2+}	$\frac{[ML]}{[M][L]}$	12.8[a]	25 °C	3.0
		10.1	37 °C	0.15
	$\frac{[ML_2]}{[M][L]^2}$	19.6[a]	25 °C	3.0
		16.89	37 °C	0.15
	$\frac{[MHL]}{[M][HL]}$	4.97[b]	25 °C	1.0
		5.35	37 °C	0.15
	$\frac{[MH_2L_2]}{[M][HL]^2}$	9.92[b]	25 °C	1.0
Hg^{2+}	$\frac{[ML]}{[M][L]}$	14.4	25 °C	0.1
	$\frac{[ML_2]}{[M][L]^2}$	42.7[c]	25 °C	1.0

Neutral cysteine is referred to as H_2L. Data are taken from Ref [70]

[a] Ref. [72]

[b] Ref. [71]

[c] Ref. [73]

nature of the interaction between the heavy metal ions, e.g., Hg(II), Cd(II), and cysteine, remains obscure. As previously noticed, experimental determination of the binding energies of cysteine and the group 12 metal ions is difficult. We previously showed that the interaction energies of solvated metal–ligand complexes by quantum mechanical calculations correlate well with experimental stability constants [78]. To examine (1) the interaction between the metal species and a neutral cysteine, (2) the difference in binding affinity of the metal ions to cysteine between the gas phase and in aqueous solution, and (3) effects of deprotonation of cysteine on binding the metal ions, the B3LYP density functional method was employed for $M(H_2cys)^{2+}$ (M = Hg, Zn, and Cd) and their deprotonated complexes, $M(Hcys)^{+}$ and M(cys) (M = Hg, Zn, and Cd) followed by their microsolvation by one or two water molecules. Note that the prescreening of all possible conformers of $Hg(H_2cys)^{2+}$ was performed with a PM3 semiempirical method in the present studies (see Sect. 2). We also examined the effects of solvent polarity of water by the CPCM method and explicit solvent effects by the addition of one or two water molecules on $M(H_2cys)^{2+}$, $M(Hcys)^{+}$, and M(cys) complexes to consider the trend of metal ion binding. Note that the interaction between tetra- or penta-hydrated metal ions and a neutral glycine and hydrated Zn^{2+} complex of a cys-containing peptide model has been examined [79, 80]. We omitted $M(Hcys)^{+}$, and M(cys) complexes without water solvation because the geometry optimization of those species leads to CO_2 dissociation. Next, we employed water microsolvation for the metal complexes with a deprotonated cysteine molecule. The microsolvation approach for amino acids, mercury species, and biochemical reactions has been used in many theoretical studies as recent examples [81–88].

2 Computational models and methods

Structures of $M(H_2cys)^{2+}$ complexes can be classified into four groups: (a) **SM** (M = Hg, Cd, and Zn), metal ion bonding with a thiolate group of a zwitterionic form of cysteine with an *N*-protonated NH_2 group; (b) **NM**: metal coordination into a NH_2 group; (c) **OM**, metal coordination into a carboxylate ion of cysteine after the deprotonation of the COOH group and the protonation of the NH_2 group; (d) **SHM**, metal coordination into a SH group. **SHM** conformers are energetically high, so we ruled out **SHM** conformers in this study. For $M(Hcys)^{+}$ complexes, first non-solvated complexes were examined on the basis of conformers of *N*,*S*, or *O*-deprotonated $M(H_2cys)^{2+}$ complexes. However, some of the conformers were decarboxylated during the geometry optimizations. Hence, we examined only water-solvated $M(OH_2)_n(Hcys)^{+}$ and $M(OH_2)_n(cys)$ (n = 1, 2) complexes. The classification of coding shown above (such as **NM** and **OM**) is not applied to deprotonated complexes.

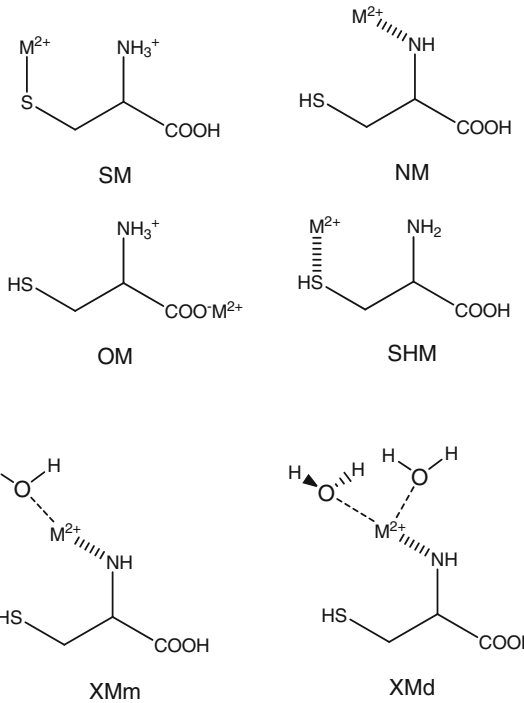

The $M(H_2cys)^{2+}$, $M(Hcys)^{+}$, and M(cys) complexes mono-coordinated by $(H_2O)_2$ (denoted as $M(OH_2)(H_2cys)^{2+}\cdot H_2O$) are marked as a complex symbol with **m**,

and $M(H_2cys)^{2+}$ and $M(Hcys)^{+}$ complexes di-coordinated by two molecules of H_2O (written as $M(OH_2)_2(H_2cys)^{2+}$) are denoted as a complex symbol with **d**.

$M(Hcys)^{+}$ and M(cys) complexes are coded after the addition of **−H** and **−2H**, respectively. The conformational analysis of $Hg(H_2cys)^{2+}$ was first performed using the PM3 semiempirical method and Spartan'04 package [89]. After the duplicated conformers were eliminated, the conformers for which energies were 200 kJ/mol higher than the most stable conformer were disregarded. Then, models of the other species were constructed on the basis of the conformational screening. The geometry optimizations based on the energy conformers were performed by the B3LYP density functional method [90] in combination with the 6-31G(d) basis sets for C, H, N, O atoms [91], a quasi-relativistic SDD effective core potential for a metal ion, and a D95(d) basis set for S (Gaussian 03 program denotes D95(d) as "SDD") denoted as basis I, for geometry optimizations. Next, the energies were computed with the 6-311++G(d,p) basis sets for C, H, N, and O atoms [92], a D95(d) basis set for S, and the SDD effective core potential [64] for a metal (with one f function, whose exponents $\alpha = 1.16$ for Hg, 1.82 for Cd, and 4.20 for Zn are optimized according to the procedure by Ehlers et al. [92]) denoted as basis II for B3LYP/I optimized conformers. The structures optimized at the B3LYP/I level are essentially the same as B3LYP/6-311+G(d,p)-LANL2DZ results shown by Russo et al. [56]. In the cases of some conformers of $M(OH_2)_n(H_2cys)^{2+}$ and $M(OH_2)_n(Hcys)^{+}$ ($n = 0, 1, 2$), B3LYP/II level optimizations were performed. The structures are very close to the B3LYP/I structures. The basis set superposition error for M-H_2cys^{2+} interaction at the B3LYP/II//B3LYP/II level through the counter-poise method [93] is found to be small (<3.6 kJ/mol). The effect of aqueous solution is examined with the COSMO polarized continuum method (CPCM) [94]. The United Atom Kohn–Sham (UAKS) cavities [95] are used for CPCM calculations.

For the most stable conformer of $M(H_2cys)^{2+}$ in the gas phase, CCSD(T)/II level single-point calculations for the B3LYP/II optimized structures were employed. The CCSD(T)/II level single-point calculations even for $M(H_2cys)^{2+}$ cost very much. For example, the single-point calculation of $Zn(H_2cys)^{2+}$ (Gaussian 03) at the CCSD(T)/II level takes 4 days 20 h CPU time at the Hitachi supercomputer SR11000. All calculations were performed using the Gaussian 03 program [96]. To analyze the orbital interactions, the NBO analysis was employed [97]. An analysis of second-order interaction energies among filled and vacant NBOs at the B3LYP/II//B3LYP/I level was performed. The interaction energy is expressed as follows:

$$E^{(2)}_{\phi\phi*} = -2\frac{\langle\phi|F|\phi*\rangle^2}{\varepsilon_{\phi*} - \varepsilon_{\phi}} \quad (1)$$

Note that $\phi/\phi*$ and F refer filled/vacant NBO and Fock matrix, respectively, and ε refers NBO energy.

Binding energies between a metal(II) ion and a neutral or deprotonated cysteine molecule are defined as differences between the electronic energies of the metal(II) ion and the optimized structures for the neutral or deprotonated cysteine molecule. Binding energies between a solvated metal(II) ion and a neutral or deprotonated cysteine molecule are differences between the electronic energies for the optimized structures of solvated metal(II) ion and the neutral or deprotonated cysteine molecule.

3 Results and discussion

3.1 $Hg(H_2cys)^{2+}$ complex

Nine representative structures of $Hg(H_2cys)^{2+}$ complexes are shown in Fig. 1. The notation of the complexes is described in detail in Sect. 2. Other conformers, for example, the 7th and 9th most stable conformers with a Hg-thiolate bond, **7SHg** and **9SHg**, respectively, are not shown in Fig. 1.

The structures obtained by Russo and co-workers are similar to our own findings (Fig. 1) [56], except for the most stable structure **1SHg**, which contains a strong Hg–S bond. The Hg–S bond in **1SHg** is located at the anti-position to the carbonyl oxygen. **1SHg** is formed by the deprotonation of the SH group of the cysteine followed by the protonation of the amino group, namely the Hg^{2+} ion interacting with a zwitterionic form. Note that this conformer has not been studied previously. The second most stable conformer **2SHg** has a slightly higher energy than **1SHg** by 1.3 kJ/mol at the B3LYP/II//B3LYP/II level. The Hg–S bond length of 2.53 Å in **1SHg** is slightly longer than that of 2.42 Å in **2SHg**. The second most stable mercury(II) thiolate structure **2SHg** has a strong Hg–S bond, and the carbonyl oxygen interacts with the mercury(II) ion. The non-chelated structure **1SHg** is a little more stable than **2SHg**, because of the interaction between the non-bonding orbital of the carbonyl oxygen and the $\sigma*$ orbital of the Hg–S bond in **1SHg** (−108 kJ/mol), as supported by the second-order perturbation method by natural bond orbital (NBO) analysis. In other words, a charge transfer from O into the Hg–S bond lengthens the Hg–S bond (the natural charges of Hg are +0.79e and +1.02e in **1SHg** and **2SHg**, and those of O are −0.48e and −0.61e, respectively). The most stable structure among those with an SH bond is **1NHg**, which possesses chelation with the carbonyl oxygen and the amino nitrogen. The energy of **1NHg** is higher in

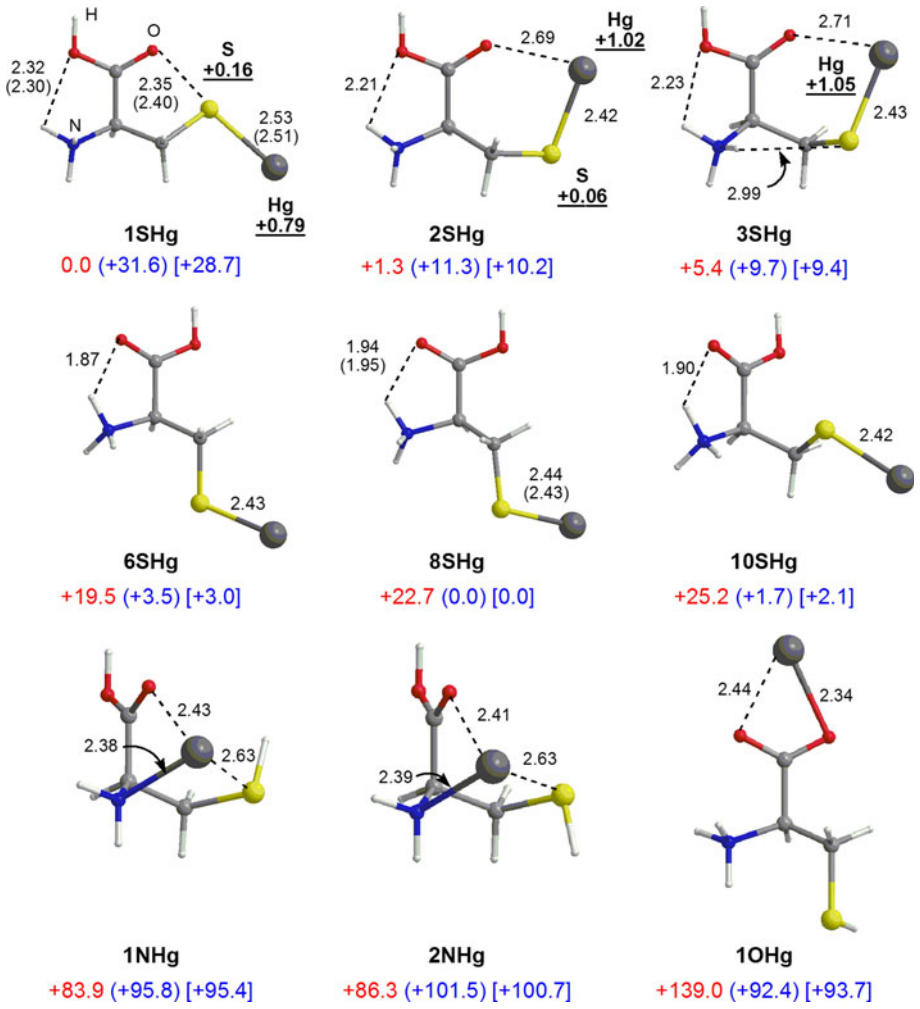

Fig. 1 Representative conformers of $Hg(H_2cys)^{2+}$. Relative energies to the most stable conformer in kJ/mol in the gas phase are shown in red at the B3LYP/II//B3LYP/I level. Relative electronic and Gibbs energies in aqueous solution to the most stable conformer are shown in *parentheses* and in *brackets* in kJ/mol at the B3LYP(CPCM)/II//B3LYP/I level, respectively. Bond lengths are in angstroms at the B3LYP/I level and in parentheses at the B3LYP/II level. Natural charges at the B3LYP/II//B3LYP/I level are *underlined*

the gas phase than **1SHg** by 83.9 and 95.4 kJ/mol (Gibbs energy) higher in the aqueous solution than **8SHg**, which is the most stable isomer under water polarity. The Hg···SH bond lengths of ca. 2.6 Å in SH-coordinated isomers are longer than those of the Hg–S bond in the thiolate-coordinated isomers. Note that in the previous studies by Russo [56]. **2NHg** is less stable in energy than the **2SHg** by 40.1 kJ/mol. The energy difference of 40.1 kJ/mol is much smaller than the difference of 85.0 kJ/mol in our current studies, probably due to the overestimation of interaction energies between a metal ion and ligands at smaller basis sets (LANL2DZ for Hg atom in the previous studies). The most stable conformer of the mercury carboxylate structure, **1OHg**, is 139 kJ/mol less stable than **1SHg** in the gas phase.

3.2 $Cd(H_2cys)^{2+}$ complex

Six representative structures of $Cd(H_2cys)^{2+}$ complexes are showed in Fig. 2. In the $Cd(H_2cys)^{2+}$ complex, the most stable structure **1SCd** has a strong Cd-S bond with chelation by a carboxylato oxygen atom both in the gas phase and in aqueous solution. The most stable structure among **NCd** conformers, **1NCd**, is less stable in energy than **1SCd** by 18.8 kJ/mol, and the energy gap between **1NCd** and **1SCd** of 18.8 kJ/mol is smaller than that between **1NHg** and **1SHg** (83.9 kJ/mol). This trend is opposite to previous studies by Russo using 6-311+G** and LANL2DZ basis sets (9.2 kJ/mol less stable in **1SCd** than **1NCd**) [56], mainly because a larger basis set superposition error appeared in the tridentate complex by using the smaller LANL2DZ basis set than the larger SDD+f basis set for Cd. In **1SCd**, the Cd charge of +1.29e is more positive than that of Hg in **2SHg** (+1.02e), indicating that Cd(II) is a harder acid than Hg(II). The **4SCd** complex, the conformation of which is related to **1SHg**, is higher in energy than **1SCd** by 34.0 kJ/mol in the gas phase and 33.2 kJ/mol under water polarity. The S-Cd bond in **4SCd** is only 0.06 Å longer than that in **1SCd**. The most stable Cd carboxylate, **1OCd**, is energetically much higher than **1SCd** by 86.6 kJ/mol in the gas phase and 41.4 kJ/mol under water polarity.

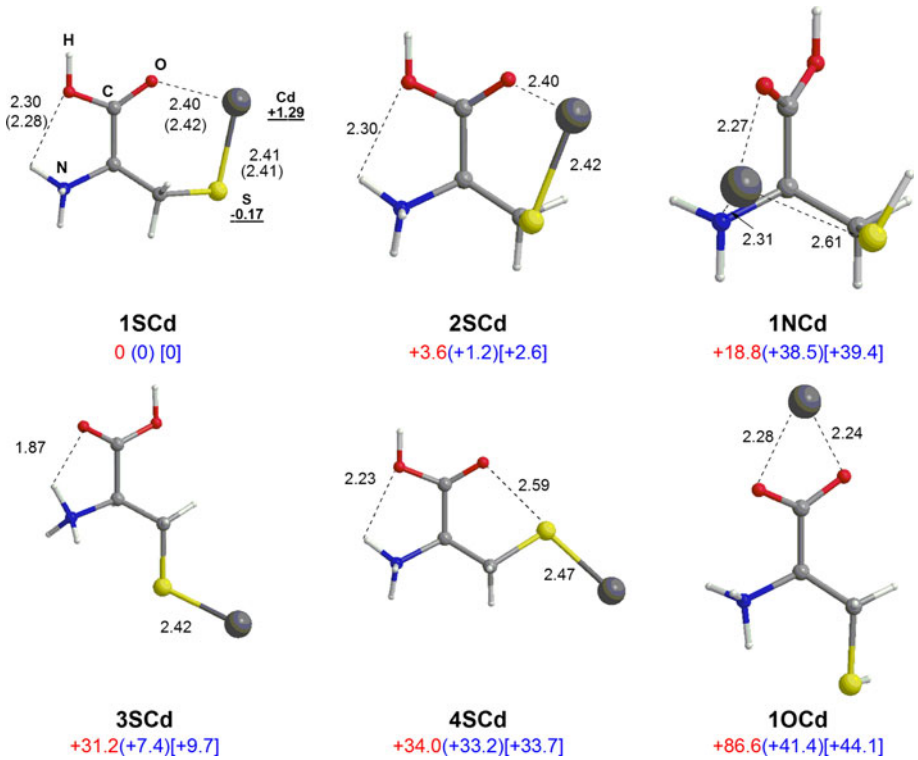

Fig. 2 Representative conformers of $Cd(H_2cys)^{2+}$. Relative energies to the most stable conformer in kJ/mol in the gas phase are shown in red at the B3LYP/II//B3LYP/I level. Relative electronic and Gibbs energies in aqueous solution to the most stable conformer are shown in *parentheses* and in *brackets* in kJ/mol at the B3LYP(CPCM)/II//B3LYP/I level, respectively. Bond lengths are in angstroms at the B3LYP/I level and in parentheses at the B3LYP/II level. Natural charges at the B3LYP/II//B3LYP/I level are *underlined*

3.3 $Zn(H_2cys)^{2+}$ complex

Six representative structures of $Zn(H_2cys)^{2+}$ complexes are showed in Fig. 3. In the $Zn(H_2cys)^{2+}$ complex, **1SZn**, an *S*-deprotonated structure with carbonyl-metal chelation is the most stable both in the gas phase and in aqueous solution. The Zn charge of +1.32e in **1SZn** is more positive than that of Cd in **1SCd**, indicating that Zn(II) is a harder acid than Hg(II) or Cd(II). Note that the Zn complex **1NZn** bearing the SH group, and without protonation of NH_2 group, is only 4.4 kJ/mol less stable than **1SZn** in the gas phase. This trend differs from the previous studies of Russo using 6-311+G(d,p) and LANL2DZ basis sets (25 kJ/mol less stable in **1SZn** than **1NZn)** [56], because a larger basis set superposition error appears in the tridentate complex at the smaller LANL2DZ basis set than the larger SDD+f basis set for Zn. In aqueous solution, **1NZn** is 39.0 kJ/mol less stable in Gibbs energy than **1SZn**. The most stable zinc carboxylate structure, **1OZn**, is 116.7 kJ/mol higher in the gas phase and 82.5 kJ/mol (Gibbs energy) higher in energy than the most stable conformer, **1SZn**. The second most stable conformer in the gas phase, **2NZn**, is a rotamer of **1NZn** with respect to the SH bond. Although the formation of a Zn carboxylate structure **OZn** seems to be highly endothermic, the probability of formation of structures other than Zn–S bond formation might be higher. The conformer, **6SZn,** in which the carbonyl oxygen is in an anti-periplanar relationship to the S–Zn bond, is 62.2 kJ/mol higher in energy than **1SZn**.

3.4 Effects of water microsolvation

Since microsolvation by water molecules is important for modeling molecular structures in solution, we carried out explicit water solvation of the $M(H_2cys)^{2+}$ and $M(Hcys)^{+}$ complexes. There are many possible coordination modes in microsolvation. We focus on explicit solvation of one or two water molecules into a metal ion to consider the metal-cysteine interaction.

3.5 $[(H_2O)Hg(H_2cys)]^{2+}$

Explicit solvation by one water molecule into $Hg(H_2cys)^{2+}$ was examined. Seven representative structures of $(H_2O)Hg(H_2cys)^{2+}$ complexes are showed in Fig. 4. We coded **aq** for one water solvation of the parent structure. The (*S*,*O*)-chelated complex **1SHgaq** is the most stable in the gas phase and is formed by monoaqua coordination of **3SHg**. The natural charge of Hg of +1.14e is a slightly more positive than that of Hg of +1.05e in **3SHg**. The O···Hg distance of 2.80 Å in **1SHgaq** is larger than that of 2.71 Å in **3SHg** (Fig. 1). The second and third most stable forms, **2SHgaq** and **3SHgaq** (**2SHgaq** is not shown), have also (*S*,*O*)-chelated complexes with different conformation. The most stable complex in aqueous solution is **6SHgaq,** which is a non-chelated structure. The coordination of a water molecule with the most stable complex, **1SHg**, in the gas phase and **8SHg** under water polarity gives **11SHgaq** and **4SHgaq**, which are 20.0 and 6.2 kJ/mol higher in

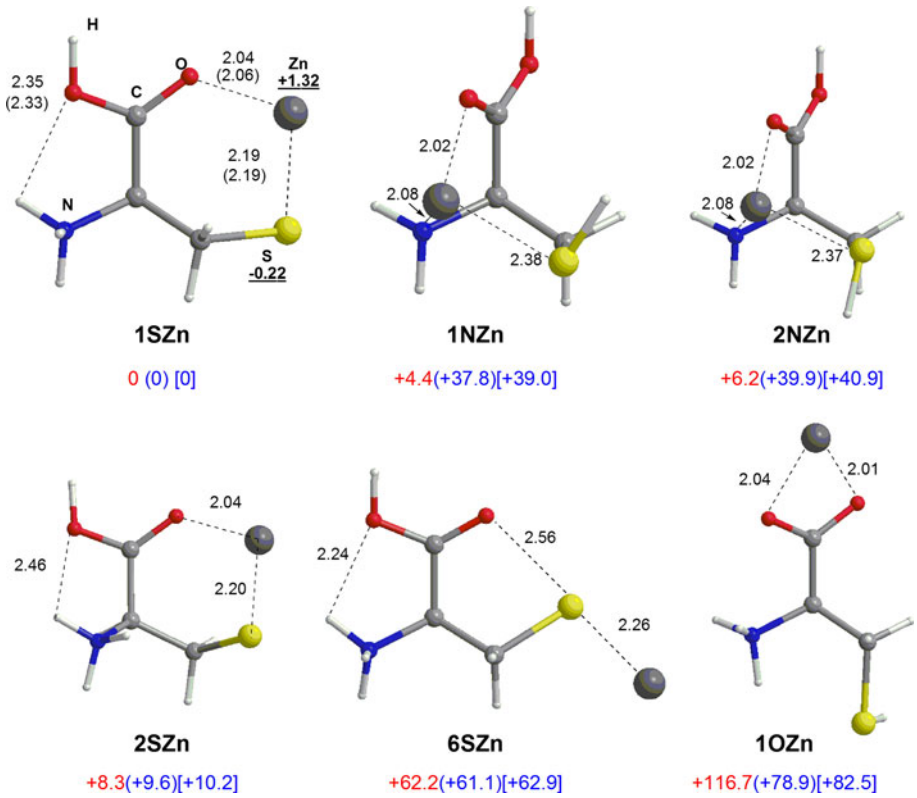

Fig. 3 Representative conformers of $Zn(H_2cys)^{2+}$. Relative energies to the most stable conformer in kJ/mol in the gas phase are shown in red at the B3LYP/II//B3LYP/I level. Relative electronic and Gibbs energies in aqueous solution to the most stable conformer are shown in *parentheses* and in *brackets* in kJ/mol at the B3LYP(CPCM)/II//B3LYP/I level, respectively. Bond lengths are in angstroms at the B3LYP/I level and in parentheses at the B3LYP/II level. Natural charges at the B3LYP/II//B3LYP/I level are *underlined*

energy than **1SHgaq** in the gas phase, respectively. The O···S atomic distance of 2.73 Å in **11SHgaq** is much longer than that of 2.35 Å in **1SHg**, indicating that water coordination loses the strong interaction between Hg and the carbonyl oxygen. The most stable Hg-NH_2-coordinated isomer, **1NHgaq**,a (*N*,*O*,*S*)-chelated complex, and the Hg(II) carboxylate species, **1OHgaq**, are higher in energy than the Hg–S bond as well as in the system of $[Hg(H_2cys)]^{2+}$. (*N*,*S*)-chelated complex without deprotonation of the SH group, **5NHgaq**, is 117.2 kJ/mol less stable than **1SHgaq**.

3.6 $[(H_2O)Cd(H_2cys)]^{2+}$

Four representative structures of $(H_2O)Cd(H_2cys)^{2+}$ complexes are showed in Fig. 5. Coordination of a water molecule into an (*O*,*S*)-chelated complex, **2SCd**, gives the most stable conformer, **1SCdaq**, in the gas phase. In **1SCdaq**, the distance between Cd and carbonyl oxygen of 2.49 Å is a little bit longer than that of 2.40 Å in **2SCd**. The most stable isomer under water polarity is **4SCdaq**, in which Cd is not chelated to the carbonyl oxygen and is higher in energy than **1SCdaq** by 18.2 kJ/mol in the gas phase. The Cd-NH_2 coordination isomer, **1NCdaq**, is higher in energy by only 9.8 kJ/mol in the gas phase, whereas it is higher in energy by 51.6 kJ/mol than **4SCdHg** under water polarity. As in non-hydrated species, the Cd charge of +1.38e in **1SCdaq** is more positive than that of Hg in **1SHgaq** of +1.14e. Cd-thiolate complexes are highly stable compared with Cd-thiol complexes. The most stable Cd carboxylate, **1OCdaq**, is 56.1 and 41.9 kJ/mol energetically less stable than the most stable complex, **1SCdaq**, in the gas phase and with water polarity, respectively. Monoaqua coordination to $[Cd(H_2cys)]^{2+}$ species does not change the fact that the Cd-thiolate structure is the most stable.

3.7 $[(H_2O)Zn(H_2cys)]^{2+}$

Coordination of one water molecule into **1NZn** gives **1NZnaq**, the most stable conformer among $[(H_2O)Zn(H_2cys)]^{2+}$ complexes in the gas phase as shown in Fig. 6. **1NZnaq** is an (*N*,*O*,*S*)-tridentate complex without deprotonation of the SH group. The distance between Zn and carbonyl oxygen in **1NZnaq** is short as 2.06 Å, and the distance between Zn and N is 2.10 Å. The most stable conformer under water polarity is **1SZnaq**, in which the carbonyl oxygen is chelated into Cd as shown in the distance between Zn and O of 2.13 Å. These results suggest that solvent polarity can control the stability between Zn(thiolate) and Zn(amine) complexes. The most stable Zn carboxylate structure, **1OZnaq**, is 70.0 kJ/mol higher in energy in the gas phase than **1NZnaq**. **1OZnaq** is 60.1 kJ/mol higher in energy than **1SZnaq**, which is the most stable species with water polarity. These results suggest that Zn carboxylate species can be ruled out from a

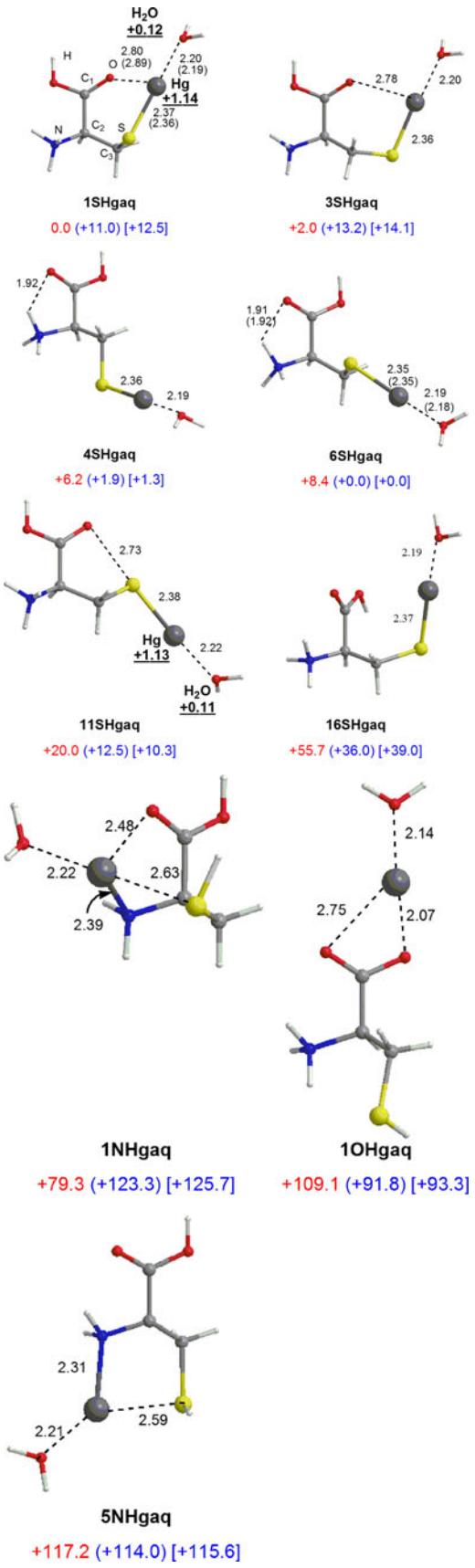

◀ **Fig. 4** Representative conformers of $(H_2O)Hg(H_2cys)^{2+}$. Relative energies to the most stable conformer in kJ/mol in the gas phase are shown in *red* at the B3LYP/II//B3LYP/I level. Relative electronic and Gibbs energies in aqueous solution to the most stable conformer are shown in *parentheses* and in *brackets* in kJ/mol at the B3LYP(CPCM)/II//B3LYP/I level, respectively. Bond lengths are in angstroms at the B3LYP/I level and in parentheses at the B3LYP/II level. Natural charges at the B3LYP/II//B3LYP/I level are *underlined*

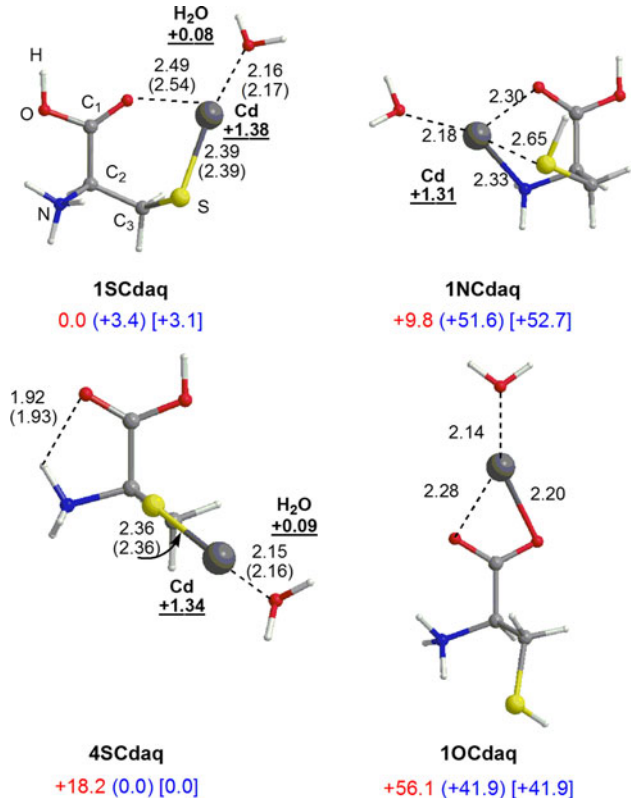

Fig. 5 Representative conformers of $(H_2O)Cd(H_2cys)^{2+}$. Relative energies to the most stable conformer in kJ/mol in the gas phase are shown in red at the B3LYP/II//B3LYP/I level. Relative electronic and Gibbs energies in aqueous solution to the most stable conformer are shown in *parentheses* and in *brackets* in kJ/mol at the B3LYP(CPCM)/II//B3LYP/I level, respectively. Bond lengths are in angstroms at the B3LYP/I level and in parentheses at the B3LYP/II level. Natural charges at the B3LYP/II//B3LYP/I level are *underlined*

possibility of the complex formation. As expected, the Zn charges of +1.55 and +1.40e in **1NZnaq** and **1SZnaq**, respectively, are more positive than that of Cd in **1SCdaq**, indicating that Zn is harder acid than Cd.

3.8 $[(H_2O)_2Hg(H_2cys)]^{2+}$

Four representative structures of diaqua-coordinated $Hg(H_2cys)^{2+}$ are shown in Fig. 7. The most stable structure in the gas phase, **1SHgm,** is formed by coordination between **1SHgaq** and one additional water molecule. The most stable structure under water polarity, **4SHgm**, is a complex between a water molecule and the most stable

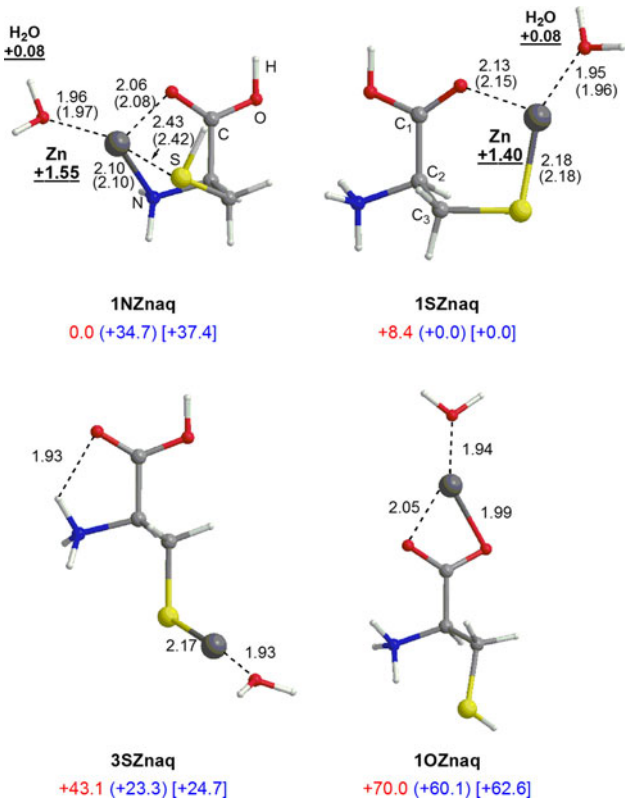

Fig. 6 Representative conformers of $(H_2O)Zn(H_2cys)^{2+}$. Relative energies to the most stable conformer in kJ/mol in the gas phase are shown in red at the B3LYP/II//B3LYP/I level. Relative electronic and Gibbs energies in aqueous solution to the most stable conformer are shown in *parentheses* and in *brackets* in kJ/mol at the B3LYP(CPCM)/II//B3LYP/I level, respectively. Bond lengths are in angstrom at the B3LYP/I level and in parentheses at the B3LYP/II level. Natural charges at the B3LYP/II//B3LYP/I level are *underlined*

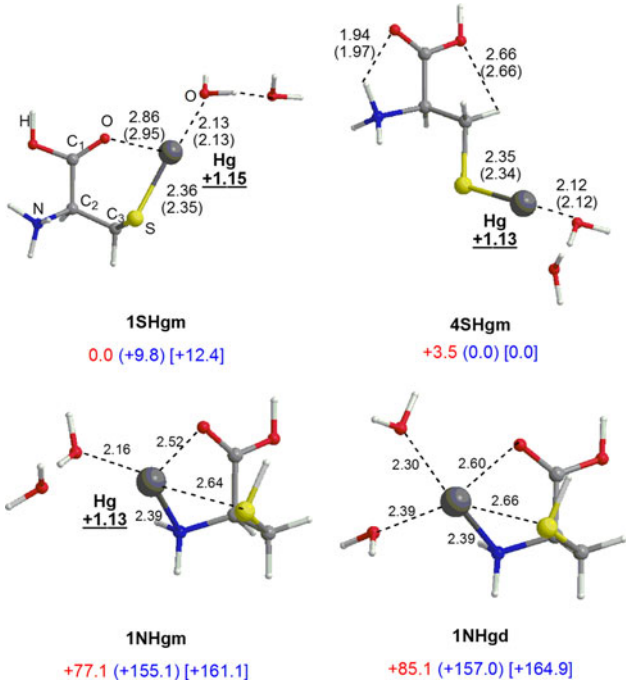

Fig. 7 Representative conformers of $(H_2O)_2Hg(H_2cys)^{2+}$. Relative energies to the most stable conformer in kJ/mol in the gas phase are shown in red at the B3LYP/II//B3LYP/I level. Relative electronic and Gibbs energies in aqueous solution to the most stable conformer are shown in *parentheses* and in *brackets* in kJ/mol at the B3LYP(CPCM)/II//B3LYP/I level, respectively. Bond lengths are in angstroms at the B3LYP/I level and in parentheses at the B3LYP/II level. Natural charges at the B3LYP/II//B3LYP/I level are *underlined*

$[(H_2O)Hg(H_2cys)]^{2+}$ structure, **4SHgaq**, under water polarity. Both structures have one water-coordinated Hg atom. The optimization of a diaqua-coordinated Hg-thiolate complex led to one water dissociation followed by strong hydrogen bonding into the other water coordinated to the Hg atom. The formula of these structures can be written as $Hg(H_2cys)(OH_2)^{2+}\cdot H_2O$ rather than $Hg(H_2cys)(OH_2)_2^{2+}$. In Hg-amine complexes, we found two types of water coordination into the Hg atom. The most stable isomers for Hg(amine) complexes, **1NHgm** and **1NHgd**, are much higher in energy (by 77.1 and 85.1 kJ/mol in the gas phase, respectively) than the most stable complex, **1SHgm**. Instability of both species is at least high as 155.0 kJ/mol in energy under water polarity. These results suggest the strong preference of a Hg-thiolate bond in the presence of a water molecule. The Hg charge in **1SHgm** of +1.15e does not change so much from that of Hg in **1NHgm**, and there is no energetically stable diaqua-coordinated Hg complex as a minimum of potential energy hypersurface, indicating that the thiolate ligand controls the direction of water coordination much more than the amine ligand.

3.9 $[(H_2O)_2Cd(H_2cys)]^{2+}$

Four representative structures of diaqua-coordinated $Cd(H_2cys)^{2+}$ are shown in Fig. 8. The most stable structure in the gas phase, **1SCdd**, has diaqua coordination at the Cd atom. The distance between the carbonyl oxygen and Cd of 2.55 Å in **1SCdd** is slightly longer than that in **1SCdaq** because of the second water solvation. The next most stable structure, **1NCdd**, exhibiting a Cd-amine coordination is only 1.8 kJ/mol less stable than **1SCdd**. The most stable structure under water polarity is **4SCdm** with monoaqua coordination. **1SCdm** is less stable than **1SCdd** by 8.2 kJ/mol in the gas phase and less stable than **4SCdm** by 6.2 kJ/mol in water polarity. The diaqua complexes **1SCdd** and **1NCdd** are higher in energy with solvent polarity than **4SCdm** by 40.2 and 62.3 kJ/mol, respectively. In this case, under water polarity, monoaqua coordination is preferred to diaqua coordination.

3.10 $[(H_2O)_2Zn(H_2cys)]^{2+}$

Five representative structures of diaqua-coordinated $Zn(H_2cys)^{2+}$ are shown in Fig. 9. The most stable structure in the gas phase, **1NZnd**, has diaqua coordination for the

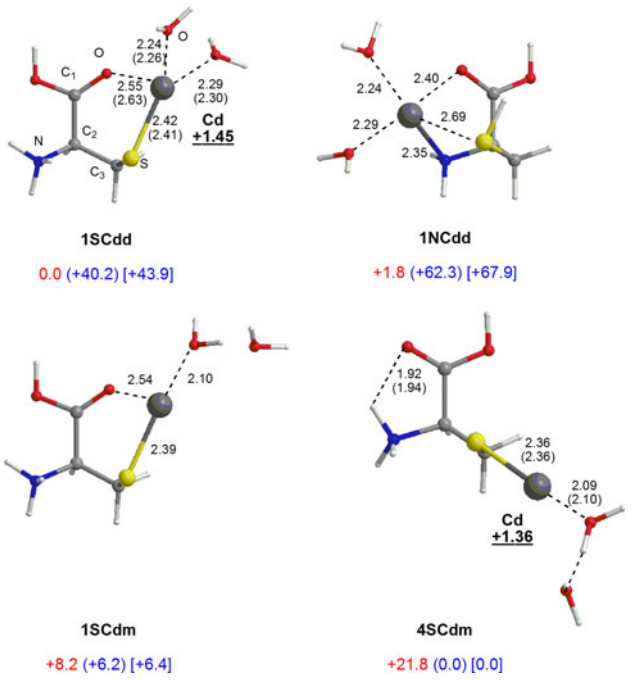

Fig. 8 Representative conformers of $(H_2O)_2Cd(H_2cys)^{2+}$. Relative energies to the most stable conformer in kJ/mol in the gas phase are shown in red at the B3LYP/II//B3LYP/I level. Relative electronic and Gibbs energies in aqueous solution to the most stable conformer are shown in *parentheses* and in *brackets* in kJ/mol at the B3LYP(CPCM)/II//B3LYP/I level, respectively. Bond lengths are in angstroms at the B3LYP/I level and in parentheses at the B3LYP/II level. Natural charges at the B3LYP/II//B3LYP/I level are *underlined*

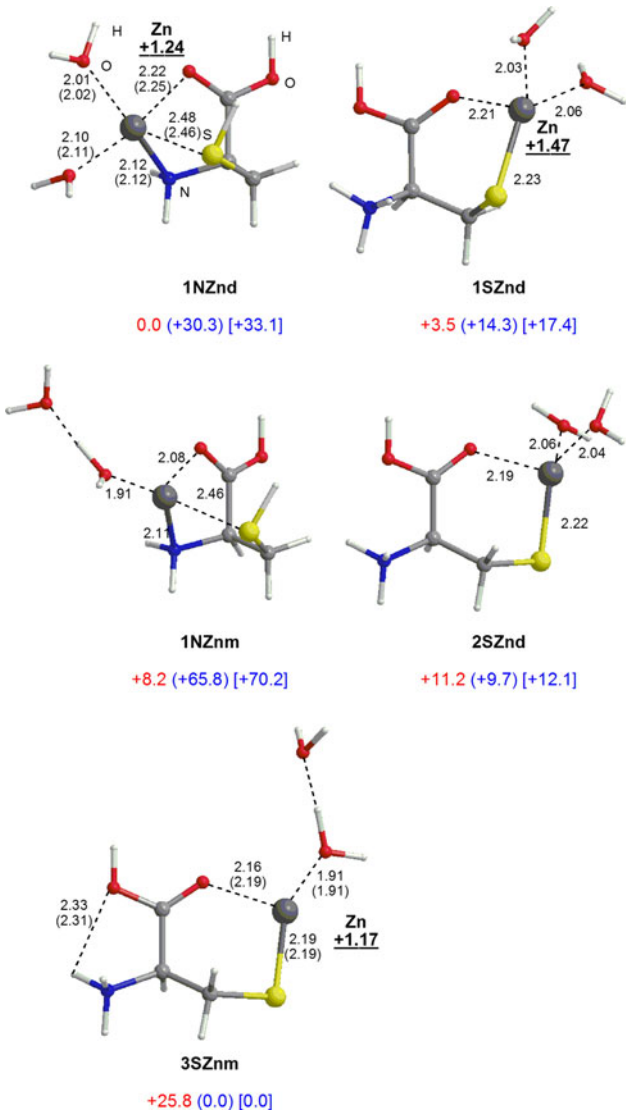

Fig. 9 Representative conformers of $(H_2O)_2Zn(H_2cys)^{2+}$. Relative energies to the most stable conformer in kJ/mol in the gas phase are shown in red at the B3LYP/II//B3LYP/I level. Relative electronic and Gibbs energies in aqueous solution to the most stable conformer are shown in *parentheses* and in *brackets* in kJ/mol at the B3LYP(CPCM)/II//B3LYP/I level, respectively. Bond lengths are in angstroms at the B3LYP/I level and in parentheses at the B3LYP/II level. Natural charges at the B3LYP/II//B3LYP/I level are *underlined*

Zn ion with an amine ligand without deprotonation of the SH group. The second most stable structure, **1SZnd**, bearing a Zn-thiolate bond with diaqua coordination, is 3.5 kJ/mol less stable than **1NZnd** in the gas phase. In the gas phase, a monoaqua complex, **1NZnm,** is less stable than its diaqua analog, **1NZnd**, by 8.2 kJ/mol. Another diaqua complex, **2SZnd**, with a Zn-thiolate bond is 11.2 kJ/mol less stable in energy than **1NZnd** in the gas phase. The most stable structure under water polarity is **3SZnm** with monoaqua coordination. The diaqua complexes, **1SZnd**, **1NZnd**, and **2SZnd,** are higher in energy with solvent polarity than **3SZnm** by 30.3, 14.3, and 9.7 kJ/mol, respectively.

3.11 Deprotonated cysteine complexes

Complexes of deprotonated cysteine with one and two water molecules, $[(H_2O)M(Hcys)]^+$ and $[(H_2O)_2M(Hcys)]^+$, respectively, were examined for greater reality of species observed in aqueous media ranging from neutral to alkaline pH. We manually extracted a proton from all the optimized $[(H_2O)M(H_2cys)]^{2+}$ and $[(H_2O)_2M(H_2cys)]^{2+}$, which are less stable than the most stable isomer by at most 100 kJ/mol in energy, and then optimized the deprotonated structures. The doubly deprotonated complexes, $[(H_2O)M(cys)]$, are also optimized after the removal of the proton from $[(H_2O)M(Hcys)]^+$ complexes.

3.12 $[(H_2O)Hg(Hcys)]^+$

Three most stable structures of $[(H_2O)Hg(Hcys)]^+$ are shown in Fig. 10. The most stable complex in the gas phase is **1Hgaq-H**, chelated by three atoms, O, S, and N. **1Hgaq-H** can be formed by deprotonation of the SH group in **1NHgaq** (Fig. 10). The chelation mode is different from

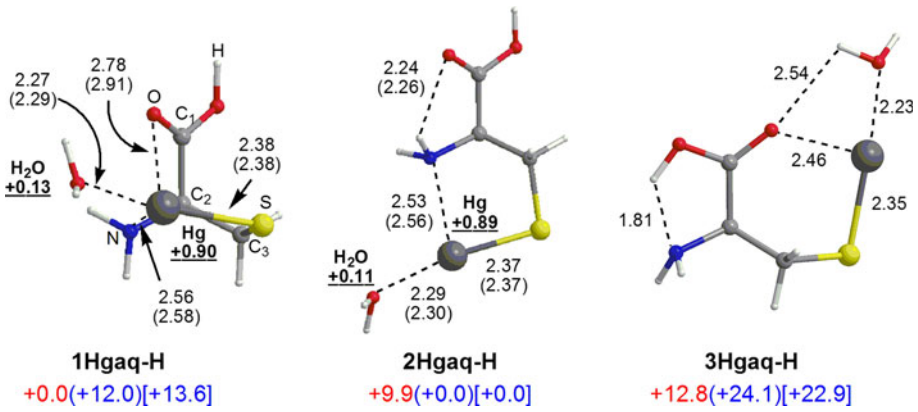

Fig. 10 Representative conformers of $(H_2O)Hg(Hcys)^+$. Relative energies to the most stable conformer in kJ/mol in the gas phase are shown in red at the B3LYP/II//B3LYP/I level. Relative electronic and Gibbs energies in aqueous solution to the most stable conformer are shown in *parentheses* and in *brackets* in kJ/mol at the B3LYP(CPCM)/II//B3LYP/I level, respectively. Bond lengths are in angstroms at the B3LYP/I level and in parentheses at the B3LYP/II level. Natural charges at the B3LYP/II//B3LYP/I level are underlined

that of the most stable non-deprotonated complex in the gas phase, **1SHgaq**, which has (*O*,*S*)-chelation. The distance between Hg and carbonyl oxygen of 2.78 Å is comparable to that of 2.80 Å in **1SHgaq** (Fig. 4). Because this species is a cationic, the natural charge of Hg of +0.90e is less negative than that in $[(H_2O)Hg(H_2cys)]^{2+}$. Under water polarity, the (*N*,*S*)-chelated conformer, **2Hgaq-H**, is most stable. In **2SHgaq-H**, hydrogen bonding between carbonyl oxygen and NH is formed. This trend of chelation mode is also different from the most stable form of the non-deprotonated complex **6SHgaq**, which has a monodentate Hg-thiolate structure. These results suggest that Hg-cysteine complexes under basic conditions favor a multichelated conformation. Another (*N*,*S*)-chelated complex, **2Hgaq-H**, is formed by the deprotonation of **5NHgaq** (see Fig. 4), which is 117.2 kJ/mol less stable in energy than **1SHgaq** in the gas phase and 114.0 kJ/mol less stable than **6SHgaq** with water polarity. An (*O*,*S*)-chelated complex, **3Hgaq-H**, is formed by removal of a proton bound to a nitrogen atom of **16SHgaq** (Fig. 4).

3.13 $[(H_2O)Cd(Hcys)]^+$

Three most stable structures of $[(H_2O)Cd(Hcys)]^+$ are shown in Fig. 11. The most stable form in the gas phase, **1Cdaq-H**, is similar to **1Hgaq-H** with respect to the (*N*,*O*,*S*)-chelation mode. The **1Cdaq-H** complex is made by the *S*-deprotonation of **1NCdaq**. The Cd charge of +1.37e in **1Cdaq-H** is more positive than that of Hg in **1Hgaq-H** of +0.90e, as expected. The second most stable complex in the gas phase, **2Cdaq-H**, is 21.3 kJ/mol less stable in energy than that of **1Cdaq-H**. **2Cdaq-H** has (*O*,*S*)-chelation. The mode of chelation for **3Cdaq-H** as (*N*,*S*)-chelation is similar to the Hg(II) analog, **2Hgaq-H**, which is in the most stable form $[(H_2O)Hg(Hcys)]^+$, with water polarity. **3Cdaq-H** is formed by the *S*-deprotonation of **5NCdaq** (data not shown), which is 70.2 kJ/mol less stable than **1SCdaq** in the gas phase and 51.8 kJ/mol less stable than **4SCdaq** with water polarity. Hydrogen bonding between oxygen and NH is formed in **3Cdaq-H**.

3.14 $[(H_2O)Zn(Hcys)]^+$

Four representative stable structures of $[(H_2O)Zn(Hcys)]^+$ are shown in Fig. 12. Both in the gas phase and in aqueous solution, the (*N*,*O*,*S*)-chelated complex, **1Znaq-H**, is most stable. The natural charge of +1.41e in **1Znaq-H** is slightly more positive than that of +1.37e in **1Cdaq-H**. The **1Znaq-H** complex is formed by the *S*-deprotonation of **1NZnaq**, which is most stable in the gas phase. The second most stable complex in the gas phase, **2Znaq-H**, is an (*O*,*S*)-chelate complex. A complex, **4Znaq-H**, is a rotamer of **1Znaq-H** with respect to the OH bond of the COOH group. The (*N*,*S*)-chelate complex, **5Znaq-H**, is only slightly higher in energy than the **1Znaq-H** complex by 0.9 kJ/mol under water polarity.

3.15 $[(H_2O)_2Hg(Hcys)]^+$

Six representative stable structures of $[(H_2O)_2Hg(Hcys)]^+$ are shown in Fig. 13. In the most stable form in the gas phase, **1Hgm-H**, one water molecule is solvated with Hg, and the carbonyl oxygen forms a hydrogen-bond network with two water molecules (Fig. 13). In **1Hgm-H**, interaction between carbonyl oxygen and Hg is very small. The second most stable complex, **2Hgm-H**, in the gas phase is similar to **1Hgm-H** except for the orientation of an OH bond in H_2O bound to Hg. The third most stable complex in the gas phase, **3Hgm-H**, has (*O*,*S*)-chelation mode. An (*N*,*S*)-chelate complex, **8Hgm-H**, is 14.8 kJ/mol less stable than **1Hgm-H** in the gas phase. An (*O*,*S*)-chelate, **12Hgm-H**, is most stable with respect to Gibbs energy with

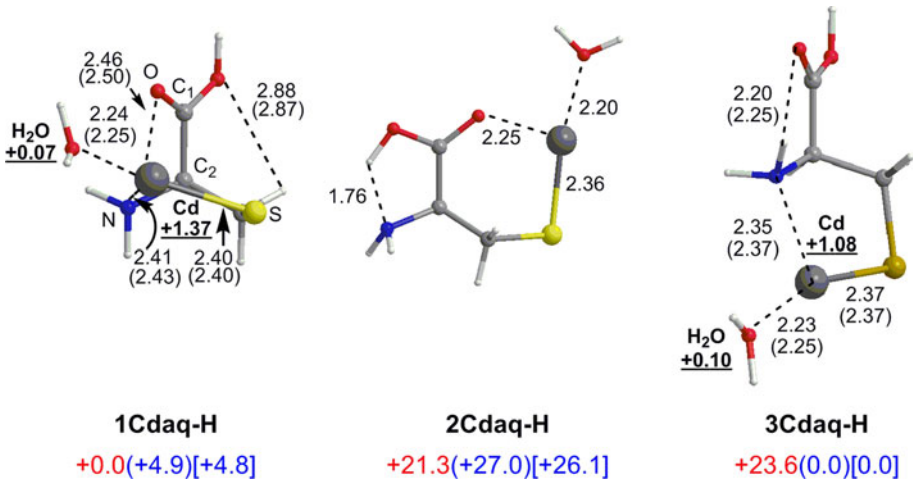

Fig. 11 Representative conformers of $(H_2O)Cd(Hcys)^+$. Relative energies to the most stable conformer in kJ/mol in the gas phase are shown in red at the B3LYP/II//B3LYP/I level. Relative electronic and Gibbs energies in aqueous solution to the most stable conformer are shown in *parentheses* and in *brackets* in kJ/mol at the B3LYP(CPCM)/II//B3LYP/I level, respectively. Bond lengths are in angstroms at the B3LYP/I level and in parentheses at the B3LYP/II level. Natural charges at the B3LYP/II//B3LYP/I level are *underlined*

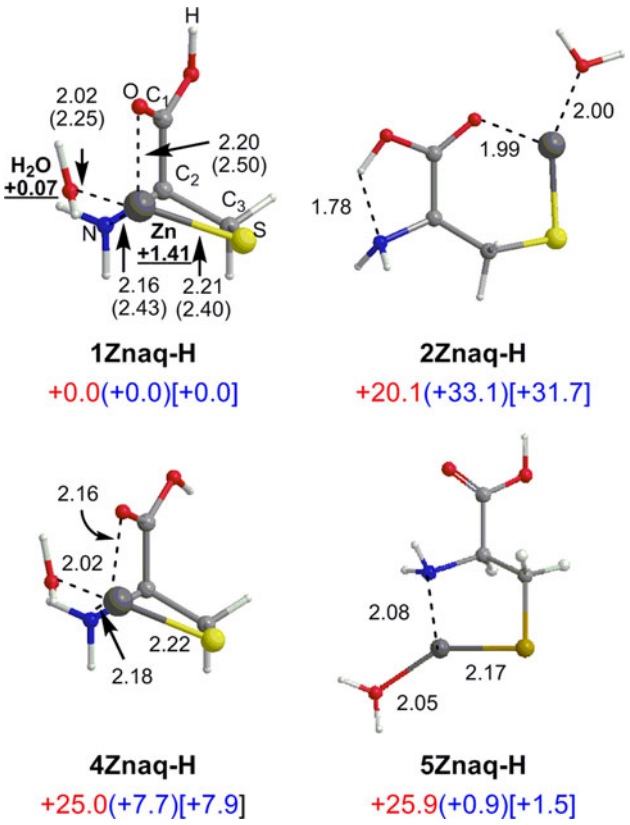

Fig. 12 Representative conformers of $(H_2O)Zn(Hcys)^+$. Relative energies to the most stable conformer in kJ/mol in the gas phase are shown in red at the B3LYP/II//B3LYP/I level. Relative electronic and Gibbs energies in aqueous solution to the most stable conformer are shown in *parentheses* and in *brackets* in kJ/mol at the B3LYP(CPCM)/II//B3LYP/I level, respectively. Bond lengths are in angstroms at the B3LYP/I level and in parentheses at the B3LYP/II level. Natural charges at the B3LYP/II//B3LYP/I level are *underlined*

water polarity. No stable isomer of diaqua Hg complexes was found in this system. In Hg-thiolate complexes, diaqua complex, diaqua-coordinate complex into Hg, cannot be located as an equilibrium structure.

3.16 $[(H_2O)_2Cd(Hcys)]^+$

Five representative stable structures of $[(H_2O)_2Cd(Hcys)]^+$ are shown in Fig. 14. The most stable complex both in the gas phase and under water polarity is **1Cdd-H**, with (*N*,*S*)-chelation. In this form, two water molecules are coordinated with a Cd(II) ion, and one water molecule bridges between Cd and the carbonyl oxygen. The most stable monoaqua complex with (*N*,*O*,*S*)-coordination, **1Cdm-H**, is 6.5 and 3.2 kJ/mol higher in energy than **1Cdd-H** in the gas phase and under water polarity, respectively. The second most stable complex, **2Cdd-H**, has (*N*,*O*,*S*)-chelation and 7.8 kJ/mol less stable than **1Cdd-H** in the gas phase and 10.5 kJ/mol in energy under water polarity.

3.17 $[(H_2O)_2Zn(Hcys)]^+$

Five representative stable structures of $[(H_2O)_2Zn(Hcys)]^+$ are shown in Fig. 15. The most stable complex both in the gas phase and with water polarity is the (*N*,*S*)-chelated diaqua Zn complex, **1Znd-H**. The most stable monoaqua Zn complex, **1Znm-H** with (*N*,*O*,*S*)-chelation is higher in energy than **1Znd-H** by 12.7 kJ/mol in the gas phase. In **1Znd-H**, one water molecule is bridging between a carbonyl oxygen and a Zn ion. The most stable (*O*,*S*)-chelated diaqua complex is **2Znd-H**, which is 21.6 kJ/mol higher

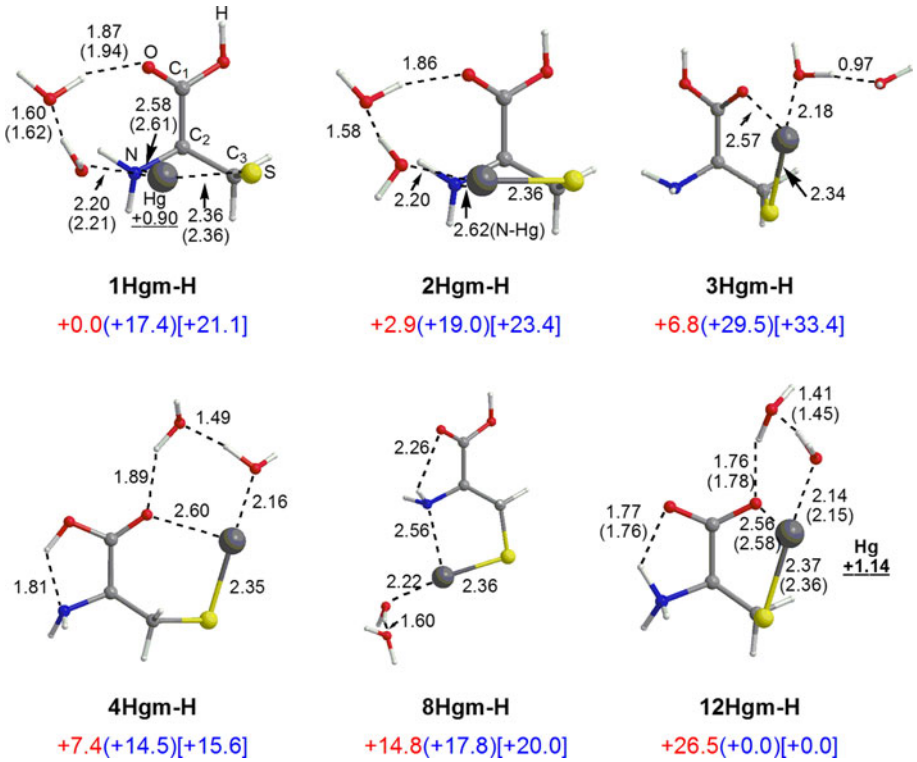

Fig. 13 Representative conformers of $(H_2O)_2Hg(Hcys)^+$. Relative energies to the most stable conformer in kJ/mol in the gas phase are shown in red at the B3LYP/II//B3LYP/I level. Relative electronic and Gibbs energies in aqueous solution to the most stable conformer are shown in *parentheses* and in *brackets* in kJ/mol at the B3LYP(CPCM)/II//B3LYP/I level, respectively. Bond lengths are in angstroms at the B3LYP/I level and in parentheses at the B3LYP/II level. Natural charges at the B3LYP/II//B3LYP/I level are *underlined*

than **1Znd-H** in the gas phase. The second most stable complex in the gas phase, **2Znm-H,** is formed by hydrogen bonding between a water molecule of **2Znaq-H** and one additional water and is 25.1 kJ/mol less stable than **1Znd-H** in the gas phase. A (*N*,*S*)-chelated diaqua Zn complex **4Znd-H**, which is led by one additional water coordination of **5Znaq-H,** is 6.6 kJ/mol less stable than **1Znd-H** with water polarity.

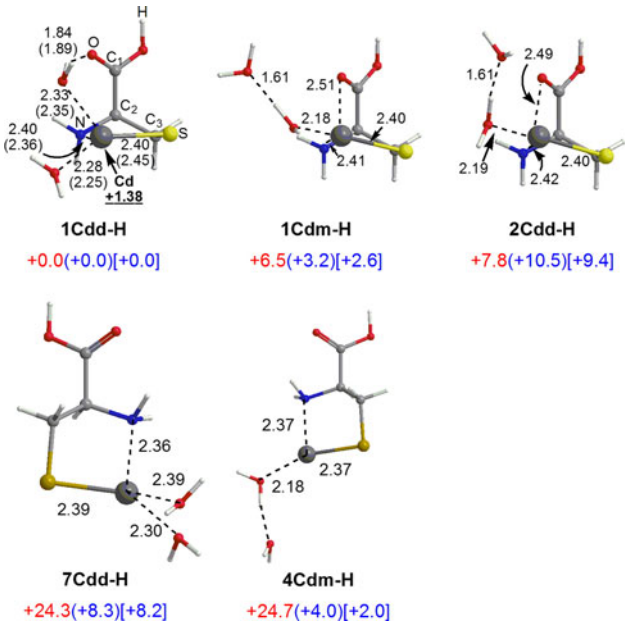

Fig. 14 Representative conformers of $(H_2O)_2Cd(Hcys)^+$. Relative energies to the most stable conformer in kJ/mol in the gas phase are shown in red at the B3LYP/II//B3LYP/I level. Relative electronic and Gibbs energies in aqueous solution to the most stable conformer are shown in *parentheses* and in *brackets* in kJ/mol at the B3LYP(CPCM)/II//B3LYP/I level, respectively. Bond lengths are in angstroms at the B3LYP/I level and in parentheses at the B3LYP/II level. Natural charges at the B3LYP/II//B3LYP/I level are *underlined*

3.18 $[(H_2O)Hg(cys)]$

Doubly deprotonated and water-solvated Hg(cys) has been examined based on proton removal from **1Hgaq-H**, **2Hgaq-H**, and **3Hgaq-H** (Fig. 16). We found that the most stable form in the gas phase, **1Hgaq-2H**, has (*N*,*O*,*S*)-chelation. A water molecule coordinated into the Hg(II) ion is also interacting with a carbonyl oxygen. An (*O*,*S*)-chelate complex, **2Hgaq-2H**, which is formed by proton removal from **3Hgaq-H** is 13.3 kJ/mol less stable in energy than **1Hgaq-2H** in the gas phase. In **2Hgaq-2H**, a water molecule interacts both with the Hg(II) ion and a carbonyl oxygen. The most stable form in aqueous solution, **3Hgaq-2H**, has (*N*,*S*)-chelation form. In the gas phase, **3Hgaq-2H** is 75.2 kJ/mol less stable in energy than that of **1Hgaq-2H**. **1Hgaq-2H** is only 6.8 kJ/mol less stable in energy than **3Hgaq-2H** with water polarity.

3.19 $[(H_2O)Cd(cys)]$

$[(H_2O)Cd(cys)]$ is examined by the removal of a proton from $[(H_2O)Cd(Hcys)]^+$ (Fig. 17). The most stable complex both in the gas phase and with water polarity is

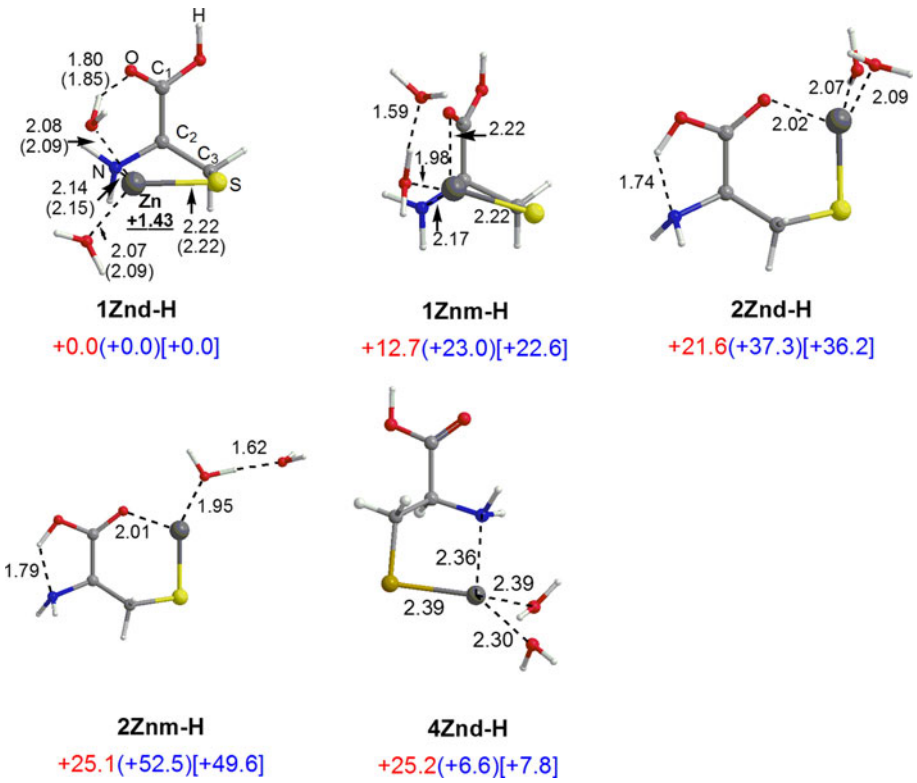

Fig. 15 Representative conformers of $(H_2O)_2Zn(Hcys)^+$. Relative energies to the most stable conformer in kJ/mol in the gas phase are shown in red at the B3LYP/II//B3LYP/I level. Relative electronic and Gibbs energies in aqueous solution to the most stable conformer are shown in *parentheses* and in *brackets* in kJ/mol at the B3LYP(CPCM)/II//B3LYP/I level, respectively. Bond lengths are in angstroms at the B3LYP/I level and in parentheses at the B3LYP/II level. Natural charges at the B3LYP/II//B3LYP/I level are *underlined*

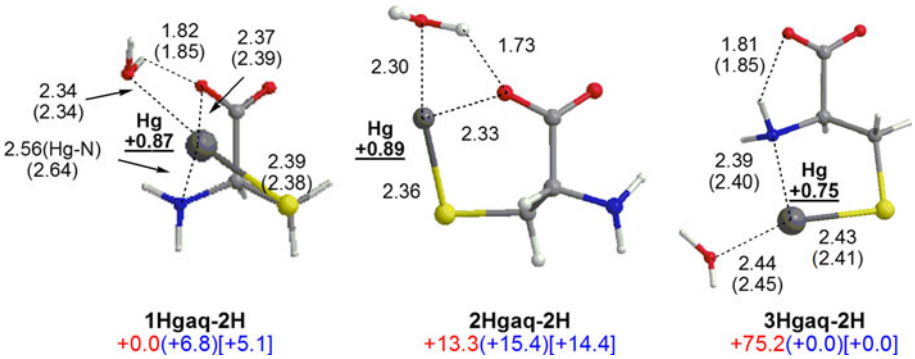

Fig. 16 Representative conformers of $(H_2O)Hg(cys)$. Relative energies to the most stable conformer in kJ/mol in the gas phase are shown in red at the B3LYP/II//B3LYP/I level. Relative electronic and Gibbs energies in aqueous solution to the most stable conformer are shown in *parentheses* and in *brackets* in kJ/mol at the B3LYP(CPCM)/II//B3LYP/I level, respectively. Bond lengths are in angstroms at the B3LYP/I level and in parentheses at the B3LYP/II level. Natural charges at the B3LYP/II//B3LYP/I level are *underlined*

1Cdaq-2H, which has (*N*,*O*,*S*)-chelation and has a water molecule coordinated to the Cd(II) ion. The natural charge of Cd in **1Cdaq-2H** of +1.05e is more positive than that of Hg in **1Hgaq-2H** of +0.87e. The distance between the carbonyl oxygen and Cd(II) ion of 2.23 Å is shorter than that between the carbonyl oxygen and Hg of 2.37 Å in **1Hgaq-2H**. Note that the fact that the van der Waals radius of Hg of 1.55 Å is almost the same as that of Cd of 1.58 Å suggests that the shorter Cd···O distance than the Hg···O distance is due to the larger affinity between Cd and the carbonyl oxygen [98]. The water molecule also interacts with an oxygen atom of the carboxylato group. An (*O*,*S*)-chelate complex, **2Cdaq-2H**, which is formed by removal of proton from **3Cdaq-H**, is 29.9 and 26.8 kJ/mol less stable than **1Cdaq-2H** in the gas phase and with water polarity, respectively. Another complex, **3Cdaq-2H**, which has a coordination mode similar to the $[(H_2O)Hg(cys)]$ complex (**1Hgaq-2H**) in the gas phase, is 106.0 kJ/mol less stable in the gas phase and 14.9 kJ/mol less stable with water polarity.

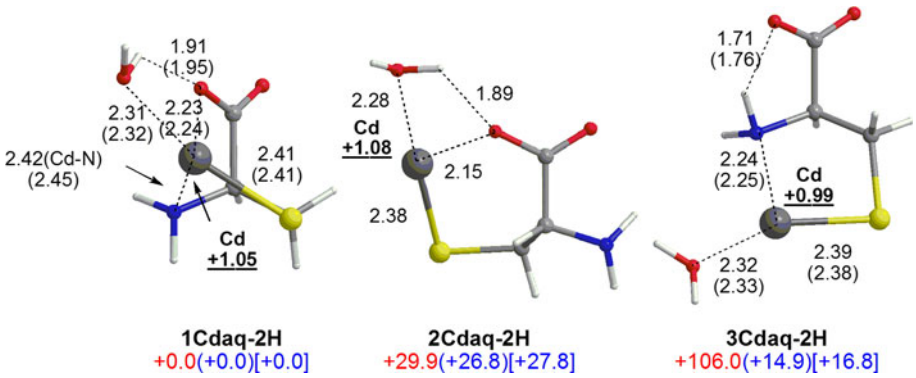

Fig. 17 Representative conformers of $(H_2O)Cd(cys)$. Relative energies to the most stable conformer in kJ/mol in the gas phase are shown in red at the B3LYP/II//B3LYP/I level. Relative electronic and Gibbs energies in aqueous solution to the most stable conformer are shown in *parentheses* and in *brackets* in kJ/mol at the B3LYP(CPCM)/II//B3LYP/I level, respectively. Bond lengths are in angstroms at the B3LYP/I level and in parentheses at the B3LYP/II level. Natural charges at the B3LYP/II//B3LYP/I level are *underlined*

3.20 $[(H_2O)Zn(cys)]$

$[(H_2O)Zn(cys)]$ was examined by the removal of a proton from $[(H_2O)Zn(Hcys)]^+$ (Fig. 18). The most stable complex both in the gas phase and with water polarity is **1Znaq-2H**, which has (*N*,*O*,*S*)-chelation and has a water molecule coordinated to the Zn(II) ion. The water molecule also interacts with an oxygen of the carboxylato group. Distance between the carbonyl oxygen and Zn of 1.98 Å is shorter than that between the carbonyl oxygen and Cd of 2.23 Å in **1Cdaq-2H**. The natural charge of Zn of +1.05e in **1Znaq-2H** is comparable to that of Cd of +1.05e in **1Cdaq-2H**. Since the van der Waals radius of Zn of 1.39 Å is smaller than that of Cd of 1.58 Å, the shorter Zn···O distance than Cd···O distance is due to the difference of the van der Waals radii. An (*O*,*S*)-chelate complex, **2Znaq-2H**, which is formed by removal of proton from **3Cdaq-H**, is 31.4 and 35.1 kJ/mol less stable than **1Znaq-2H** in the gas phase and with water polarity, respectively. Another complex, **3Znaq-2H**, which has coordination mode similar to the most stable $[(H_2O)Hg(cys)]$ complex, **3Hgaq-2H**, in the gas phase, is 116.2 kJ/mol less stable in the gas phase and 37.8 kJ/mol less stable with water polarity. The preferred coordination mode for the $[(H_2O)Zn(cys)]$ complex is similar to that for the $[(H_2O)Cd(cys)]$ complex.

3.21 $[(H_2O)_2M(cys)]$

Geometry optimizations of double hydration for M(cys) species were also performed on the basis of stable forms of $(H_2O)M(cys)$ species shown in Figs. 16, 17, 18. The most stable species of $(H_2O)_2M(cys)$ (M = Hg, Cd, and Zn) both in the gas phase and with water polarity are shown in Fig. 19. In any metallic species, the most stable one has common features of the (*N*,*O*,*S*)-chelation form as the most stable form of the $(H_2O)M(cys)$ species (Figs. 16, 17, and 18). Geometry optimization of the structure upon addition of one water molecule into monoaqua (*N*,*S*)-chelated complex **3Hgaq-2H**, which is the most stable form of $(H_2O)Hg(cys)$ with water polarity, leads (*N*,*O*,*S*)-chelation.

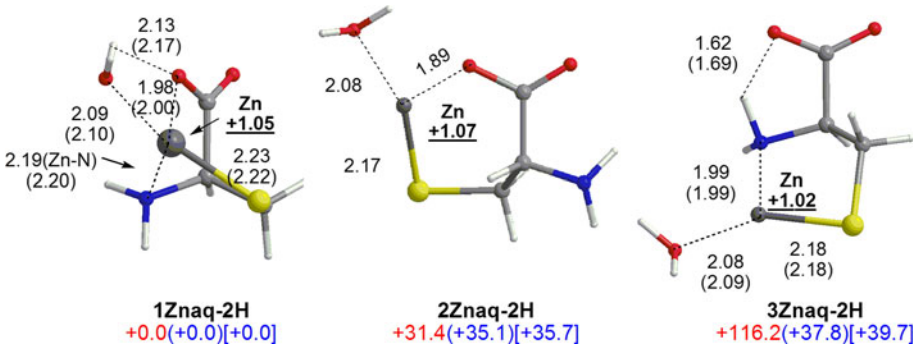

Fig. 18 Representative conformers of $(H_2O)Zn(cys)^+$. Relative energies to the most stable conformer in kJ/mol in the gas phase are shown in red at the B3LYP/II//B3LYP/I level. Relative electronic and Gibbs energies in aqueous solution to the most stable conformer are shown in *parentheses* and in *brackets* in kJ/mol at the B3LYP(CPCM)/II//B3LYP/I level, respectively. Bond lengths are in angstroms at the B3LYP/I level and in parentheses at the B3LYP/II level. Natural charges at the B3LYP/II//B3LYP/I level are *underlined*

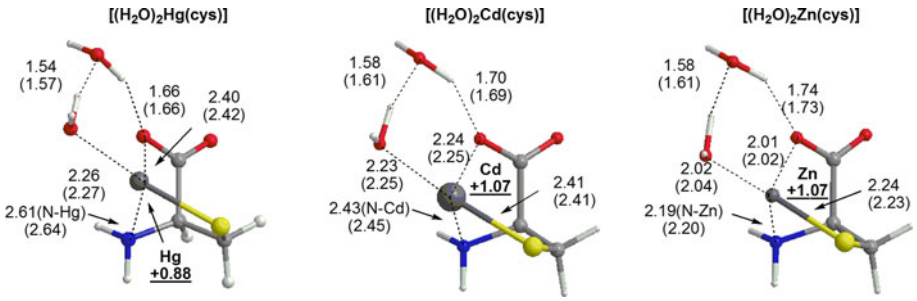

Fig. 19 Most stable conformers of $(H_2O)_2M(cys)$ (M = Hg, Cd, and Zn). Bond lengths are in angstroms at the B3LYP/I level and in parentheses at the B3LYP/II level. Natural charges at the B3LYP/II//B3LYP/I level are *underlined*

As well as in $(H_2O)M(cys)$ species, the most stable form of $(H_2O)_2M(cys)$ has (*N*,*O*,*S*)-chelation. In any structures of $(H_2O)_2M(cys)$, two water molecules were bridging between metal and oxygen by hydrogen bonding in those structures to stabilize the carboxylato group.

3.22 Binding energies

We examined the $M(H_2O)_n^{2+}$–H_2cys (M = Hg, Cd, and Zn) binding energies on the basis of the most stable isomers of cysteine and $M(H_2cys)(H_2O)_n^{2+}$ complexes in the gas phase and with water polarity, as shown in Table 2. In the case of $n = 0$, single-point energies at the CCSD(T)/II level for the B3LYP/II geometries were employed. The reference of the $M(H_2O)_n^{2+}$ ($n = 2$) is a diaqua-coordinated metal ion. According to Table 2, binding energy between a non-solvated M(II) ion and a cysteine at the B3LYP/II//B3LYP/II level is the following order: Zn(II) > Hg(II) > Cd(II). This trend is in agreement with that in previous theoretical studies [56], even though we newly found the most stable conformer in $Hg(H_2cys)^{2+}$ complex in the gas phase. The order of the binding energies at the state-of-the-art CCSD(T)/II//B3LYP/II level does not change, although the magnitude of the binding energies at the B3LYP is larger than CCSD(T) values. The trend of the binding energies at the CPCM energies with zero ionic strength and with ionic strength of 0.1 does not alter very much in the $M(H_2cys)^{2+}$ (M = Zn, Hg, and Cd) system. This is not consistent with the order of softness of the metal ions ($Hg^{2+} > Cd^{2+} > Zn^{2+}$) previously reported [99]. Zn^{2+} is higher binding affinity with the neutral cysteine than Hg^{2+} in the gas phase.[56] Next, we decided to add one or two water molecules to the metal ion and $M(H_2cys)^{2+}$ complex. If one water molecule is added, the trend of the binding energy does not change. In the case of $M(H_2cys)^{2+}$ with two H_2O molecules, the order is changed to the experimental order Table 3.

To examine the reason for the change in the order of the binding energies of metal ion-H_2cys complexes through diaqua solvation, we computed the deformation energy difference between the fragment of $[M(OH_2)\cdot H_2O]^{2+}$ (B_F) in the $M(H_2cys)^{2+}$ complex and optimized diaqua $[M(OH_2)_2]^{2+}$ (B) as expressed as $\Delta E_{def}(B) = E(B_F) - E(B)$. E refers the electronic energy of each optimized species. The fragment B_F has a monoaqua metal ion, in which the metal-coordinated water molecule interacts with another water molecule.

The deformation energies, $\Delta E_{def}(B)$, for Hg^{2+} and Cd^{2+} are +148 and 135 kJ/mol in the gas phase, respectively, and by +80 and +79 kJ/mol with water polarity, respectively. The $\Delta E_{def}(B)$ for Zn^{2+} is +194 and by +139 kJ/mol(+142 kJ/mol: Gibbs energy) in aqueous solution, which is greater than those for Hg^{2+} and Cd^{2+}. These results suggest that the higher energetic instability of the $[M(H_2O)_2]^{2+}$ in the Zn(II) complex than Hg(II) and Cd(II) complexes by interacting with a cysteine molecule affects the order of binding energies, then lowering magnitude of the binding energy for Zn(II) than Hg(II) and Cd(II) complexes by the microsolvation.

Table 2 Binding energy between a metal ion/a solvated metal ion and a neutral cysteine molecule in kJ/mol

M	B3LYP/II //B3LYP/II	CCSD(T)/II //B3LYP/II	B3LYP(CPCM)/II //B3LYP/II
Hg^{2+}	−997	−925	−209
Cd^{2+}	−837	−776	−154
Zn^{2+}	−1,026	−946	−288
$Hg(H_2O)^{2+}$	−784		−128
$Cd(H_2O)^{2+}$	−675		−80
$Zn(H_2O)^{2+}$	−798		−166
$Hg(H_2O)_2^{2+}$	−546		−125
$Cd(H_2O)_2^{2+}$	−480		−67
$Zn(H_2O)_2^{2+}$	−535		−68

The energies shown for the energy of the most stable conformer of $M(H_2cys)(H_2O)_n^{2+}$ and M^{2+}

Table 3 Deformation energy difference ΔE_{def}(B) in kJ/mol at the B3LYP/II//B3LYP/I level

	Gas phase	CPCM	CPCM (Gibbs)
Hg^{2+}	+148	+80	+82
Cd^{2+}	+135	+79	+81
Zn^{2+}	+194	+139	+142

In Table 4, we also listed the formation energies of metal-cysteine complexes based on hexaaqua-coordinated metal ions and cysteine or deprotonated cysteines (See Eq. (2); $A = H_2cys$, $Hcys^-$, cys^{2-}). The formation energy ΔE is given by Eq. (3). Hexaqua ion species are more realistic in aqueous solution [100]. In this case, hexaaquamercury(II) ion is found to bind H_2cys more strongly than hexaaquacadmium(II) and hexaaquazinc(II) ions. Some formation energies are positive (see Table 4(i)), because the energies are calculated based on infinitely separated species. In any cases, in the gas phase, Zn species show slightly stronger cysteine affinity than Cd species, but with water polarity, Cd species show a little bit stronger than Zn species. Thus, the cysteine affinities for Cd and Zn are comparable.

$$\left[M(H_2O)_6\right]^{2+} + A \rightarrow \left[M(H_2O)_nA\right]^{2+} + (H_2O)_{6-n} \quad (2)$$

$$\Delta E = E\left(\left[M(H_2O)_nA\right]^{2+}\right) + E\left((H_2O)_{6-n}\right) - E\left(\left[M(H_2O)_6\right]^{2+}\right) - E(A) \quad (3)$$

4 Conclusion

The most stable structure of $Hg(H_2cys)^{2+}$ bears a strong chelation between the carbonyl oxygen and the sulfur atom. Hg prefers to bind to S rather than N due to its softness and the atomic size of the counterpart. In the gas phase, the order of the M-H_2cys^{2+} binding energies decreases in the following order: Zn(II) > Hg(II) > Cd(II), according to both state-of-the-art CCSD(T) and B3LYP calculations. In the aqueous phase, Hg(II) > Zn(II) ~ Cd(II) through the inclusion of microsolvation effects. The CPCM calculations for systems without explicit water molecules cannot reproduce the tendency. The order of the binding energies between metallic ion and deprotonated cysteine species ($Hcys^-$ and cys^{2-}) decreases in the order: Hg(II) > Zn(II) ~ Cd(II), which in good accord with metal toxicity [50, 101]. The most stable structures of $M(H_2O)^{2+}$ complexes with $Hcys^-$, and cys^{2-} favor (*N*,*S*)- or (*N*,*O*,*S*)-chelation. Previous studies by Lewis et al. demonstrate that redox potential of metals correlates well with acute toxicity in the mouse, and the factors for the toxicity are not governed only by the LUMO energy of metal ion itself or softness of the metal ion but also by the surrounding such as water and biomolecules [102]. Microsolvation is necessary to predict interaction energies between a metal ion and cysteine molecules in aqueous solution in the present studies. The mechanism of the deprotonation of a cysteine molecule by water and molecular dynamics (MD) simulation in a water solvent box are the subject of the future studies. The current theoretical studies offer basic information for not only computational chemistry but also toxicology and environmental chemistry.

Table 4 Formation energies of aquametal ion-cysteine or deprotonated cysteine complexes in kJ/mol in Eq. (2)

M	*n*	B3LYP/II //B3LYP/II	B3LYP(CPCM)/II //B3LYP/II
(i) $A = H_2cys$			
$Hg(H_2O)^{2+}$	1	−92	−188
$Cd(H_2O)^{2+}$	1	59	−30
$Zn(H_2O)^{2+}$	1	65	16
$Hg(H_2O)_2^{2+}$	2	−151	−218
$Cd(H_2O)_2^{2+}$	2	−5	−60
$Zn(H_2O)_2^{2+}$	2	−7	8
(ii) $A = Hcys^-$			
$Hg(H_2O)^{2+}$	1	−1,877	−1,168
$Cd(H_2O)^{2+}$	1	−1,744	−1,026
$Zn(H_2O)^{2+}$	1	−1,759	−1,002
$Hg(H_2O)_2^{2+}$	2	−1,910	−1,190
$Cd(H_2O)_2^{2+}$	2	−1,773	−1,032
$Zn(H_2O)_2^{2+}$	2	−1,796	−1,028
(iii) $A = cys^{2-}$			
$Hg(H_2O)^{2+}$	1	−1,682	−262.1
$Cd(H_2O)^{2+}$	1	−1,561	−139.0
$Zn(H_2O)^{2+}$	1	−1,596	−134.0
$Hg(H_2O)_2^{2+}$	2	−1,714	−277.4
$Cd(H_2O)_2^{2+}$	2	−1,597	−160.1
$Zn(H_2O)_2^{2+}$	2	−1,633	−154.1

Acknowledgments This work was supported by Grants-in-Aid No. 19550004 for Scientific Research from JSPS and by Scientific Research on Priority Areas "Molecular Theory for Real Systems", No. 20038005 from MEXT. The generous allotment of computation time from the Research Center for Computational Science (RCCS), the National Institutes of Natural Sciences, Japan, is also gratefully acknowledged.

References

1. Zalups RK, Koropatnick J (eds) (2000) Molecular biology and toxicology of metals. Taylor & Francis, London
2. Walsh CT, Distefano MD, Moore MJ, Shewchuk LM, Verdine G (1988) FASEB J 2:124–130
3. Klaassen CD (ed) (2001) Casarett and Doull's toxicology, 6th edn
4. Steele RA, Opella SJ (1997) Biochemistry 36:6885–6895
5. Lafrance-Vanasse J, Lefebvre M, Di Lello P, Sygusch J, Omichinski JG (2009) J Biol Chem 284:938–944
6. de Montellano PRO (ed) (2005) Cytochrome P450. Kluwer/Academic/Plenum, New York
7. Choe Y-K, Nagase S (2005) J Comput Chem 26:1600–1611
8. Yanai TK, Mori S (2008) Chem Asian J 3:1900–1911
9. Yanai TK, Mori S (2009) Chem Eur J 15:4464–4473
10. Chan J, Huang Z, Merrifield ME, Salgado MT, Stillman MJ (2002) Coord Chem Rev 233–234:319–339
11. Henkel G, Krebs B (2004) Chem Rev 104:801–824
12. Stillman MJ, Shaw CF III, Suzuki KT (eds) (1991) Metallothioneins. VCH, New York
13. Zalups RK, Barfuss DW (1996) Toxicology 109:15–29
14. Oyama Y, Nakata M, Sakamoto M, Chikahisa L, Miyoshi N, Satoh M (1998) Environ Toxicol Pharmacol 6:221–227
15. Zalups RK, Barfuss DW (1995) J Toxicol Environ Health 44:401–413
16. Bridges CC, Zalups RK (2010) J. Toxicol Environ Health Part B 13:385–410
17. Clarkson TW, Magos L (2006) Crit Rev Toxicol 36:609–662
18. Aschner M, Clarkson TW (1988) Brain Res 462:31–39
19. Hirayama K (1980) Toxicol Appl Pharmocol 55:318–323
20. Kerr KA, Ashmore JP, Koetzle TF (1975) Acta Cryst B31:2022–2026
21. Noguera M, Rodríguez-Santiago L, Sodupe M, Bertran J (2001) J Mol Struct (THEOCHEM) 537:307–318
22. Fernández-Ramos A, Cabaleiro-Lagoa E, Hermida-Ramóna JM, Martínez-Núñeza E, Peña-Gallegoa A (2000) J Mol Struct (THEOCHEM) 498:191–200
23. Pecul M (2006) Chem Phys Lett 418:1–10
24. Sanz ME, Blanco S, López JC, Alonso JL (2008) Angew Chem Int Ed 47:6216–6220
25. Taylor NJ, Wong YS, Chieh PC, Carty AJ (1975) J Chem Soc Dalton Trans 438–442
26. Taylor NJ, Carty AJ (1977) J Am Chem Soc 99:6143–6145
27. Katono Y, Inoue Y, Chujo R (1977) Polym J 9:471–478
28. Natusch DFS, Porter LJ (1971) J Chem Soc A 2527–2535
29. Rubius FM, Verduci C, Giampiccolo R, Pulvirenti S, Brambilla G, Colombi A (2004) J Am Soc Mass Spectrom 15:288–300
30. Cheesman BV, Arnold AP, Rabenstein DL (1988) J Am Chem Soc 110:6359–6364
31. Jalilehvand F, Leung BO, Izadifard M, Damian E (2006) Inorg Chem 45:66–73
32. Leung BO, Jalilehvand F, Szilagyi RK (2008) J Phys Chem B 112:4770–4778
33. Hughes W Jr (1947) J Am Chem Soc 69:1836–1837
34. Nriagu JO (ed) (1979) The biogeochemistry of mercury in the environment. Elsevier/North-Holland Biomedical Press, Amsterdam
35. Oram PD, Fang X, Fernando Q, Letkeman P, Letkeman D (1996) Chem Res Toxicol 9:709–712
36. Fuhr BJ, Rabenstein DL (1973) J Am Chem Soc 95:6944–6950
37. Mah V, Jalilehvand F (2010) Chem Res Toxicol 23:1815–1823
38. Tarbouriech N, Curran J, Ruigrok RWH, Burmeister WP (2000) Nat Struct Biol 7: 777–781. 1EZJ in Protein Data Bank
39. Zalups RK, Barfuss DW (2002) J Toxicol Environ Health Part A 65:1471–1490
40. Martelli A, Rousselet E, Dyeke C, Bouron A, Moulis J-M (2006) Biochimie 88:1807–1814
41. Bottari E, Festa MR (1997) Talanta 44:1705–1718
42. Jalilehvand F, Mah V, Leung BO, Mink J, Bernard GM, Hajba L (2009) Inorg Chem 48:4219–4230
43. Barglik-Chory C, Remenyi C, Strohm H, Müller G (2004) J Phys Chem B 108:7637–7640
44. Cai Z-X, Yang H, Zhang Y, Yan X-P (2006) Anal Chim Acta 559:234–239
45. Plapp BV, Eklund H, Jones TA, Branden CI (1983) J Biol Chem 258:5537–5547
46. Ramaswamy S, Eklund H, Plapp BV (1994) Biochemistry 33:5230–5237
47. Agarwal PK, Webb SP, Hammes-Schiffer S (2000) J Am Chem Soc 122:4803–4812
48. Christianson DW, Lipscomb WN (1986) Proc Natl Acad Sci USA 83:7568–7572
49. Cameron AD, Ridderstrom M, Olin B, Kavarana MJ, Creighton DJ, Mannervik B (1999) Biochemistry 38:13480–13490
50. Venugopal B, Luckey TD (1978) Metal toxicity in mammals 2, chemical toxicity of metals and metalloids. Plenum Press, New York, USA
51. Cerda BA, Wesdemiotis C (1995) J Am Chem Soc 117:9734–9739
52. Hoyau S, Ohanessian G (1997) J Am Chem Soc 119:2016–2024
53. Zimmermann T, Zeizinger M, Burda JV (2005) J Inorg Biochem 99:2184–2196
54. Spezia R, Tournois G, Cartailler T, Tortajada J, Jeanvoine Y (2006) J Phys Chem A 110:9727–9735
55. Hay PJ, Wadt WR (1985) J Chem Phys 82:299–310
56. Belcastro M, Marino T, Russo N, Toscano M (2005) J Mass Spectr 40:300–306
57. Mori S, Kishi T, Endoh T (2004) 30th annual meeting of the society of toxicology of Japan, Sagamihara, Japan
58. Mori S, Kishi T, Endoh T, Sudou K (2004) 84th annual meeting of Chemical Society of Japan, Nishinomiya, Japan
59. Mori S, Endoh T, Kishi T (2004) 7th international conference on mercury as a global pollutant, Ljubljana, Slovenia
60. Hoffmeyer RE, Singh SP, Doonan CJ, Ross ARS, Hughes RJ, Pickering IJ, George GN (2006) Chem Res Toxicol 19:753–759
61. Bridges CC, Zalups RK (2006) Chem Res Toxicol 19:1117–1118
62. Hoffmeyer RE, Singh SP, Doonan CJ, Pickering IJ, George GN, Ross ARS, Hughes RJ (2006) Chem Res Toxicol 19:1118–1120
63. Krupp EM, Miline BF, Mestrot A, Meharg AA, Feldmann J (2008) Anal Bioanal Chem 390:1753–1766
64. Bergner A, Dolg M, Kuechle W, Stoll H, Preuss H (1993) Mol Phys 80:1431–1441
65. Ramírez J-Z, Vargas R, Garza J, Hay BP (2006) J Chem Theory Comput 2:1510–1519
66. Gourlaouen C, Piquemak J-P, Saue T, Parisel O (2005) J Comput Chem 27:142–156
67. Stricks W, Kolthoff IM (1953) J Am Chem Soc 75:5673–5681
68. Walker MD, Williams DR (1974) J Chem Soc Dalton Trans 1186–1189

69. Lenz GR, Martell AE (1964) Biochemistry 3:745–750
70. Smith RM, Martell AE (2003) NIST critically selected stability constants of metal complexes database, Version 7.0
71. Bottari E, Festa MR (1997) Talanta 44:1705–1718
72. Starý J, Kratzer K (1988) J Radioanal Nucl Chem Lett 126:69–75
73. Berthon G (1995) Pure Appl Chem 67:1117–1240
74. Rulíšek L, Havlas Z (2002) J Phys Chem A 106:3855–3866
75. Sousa SF, Fernandes PA, Ramos MJ (2007) J Phys Chem B 111:9146–9152
76. Tai H-C, Lim C (2006) J Phys Chem A 110:452–462
77. Dimakis N, Farooqi MJ, Garza ES, Bunker G (2008) J Chem Phys 128:115104
78. Ishimori K-i, Mori S, Ito Y, Ohashi K, Imura H (2009) Talanta 78:1272–1279
79. Marino T, Toscano M, Russo N, Grand A (2006) J Phys Chem B 110:24666–24673
80. Dudev T, Lim C (2007) J Am Chem Soc 129:12497–12504
81. Schmitt M, Böhm M, Ratzer C, Vu C, Kalkman I, Meerts WL (2005) J Am Chem Soc 127:10356–10364
82. Ahn D-S, Park S-W, Jeon I-S, Lee M-K, Kim N-H, Han Y-H, Lee S (2003) J Phys Chem B 107:14109–14118
83. Michaux C, Wouters J, Perpete EA, Jacquemin D (2008) J Phys Chem B 112:9896–9902
84. Bachrach SM, Nguyen TT, Demoin DW (2009) J Phys Chem A 113:6172–6181
85. Moisés CL, Ramos DR, Santaballa JA (2006) Chem Phys Lett 417:28–33
86. Rai AK, Fei W, Lu Z, Lin Z (2009) Theor Chem Acc 124:37–47
87. Gao B, Wyttenbach T, Bowers MT (2009) J Am Chem Soc 131:4695–4701
88. Shepler BC, Wright AD, Balabanov NB, Peterson KA (2007) J Phys Chem A 111:11342–11349
89. Spartan'04, Wavefuntion Inc, Irvine
90. See Cramer CJ (2002) Essentials of computational chemistry. Wiley, Chichester
91. Hehre WJ, Radom L, Schleyer PvR, Pople JA (1986) Ab initio molecular orbital theory. John Wiley, New York
92. Ehlers AW, Böhme M, Dapprich S, Gobbi A, Höllwarth A, Jonas V, Köhler KF, Stegmann R, Veldkamp A, Frenking G (1993) Chem Phys Lett 208:111–114
93. Boys SF, Bernardi F (1970) Mol Phys 19:553–566
94. Barone V, Cossi M (1998) J Phys Chem A 102:1995–2001
95. Takano Y, Houk KN (2005) J Chem Theory Comput 1:70–77
96. Gaussian 03, Revision B.03, Frisch MJ, Trucks GW, Schlegel HB, Scuseria GE, Robb MA, Cheeseman JR, Montgomery JA Jr, Vreven T, Kudin KN, Burant JC, Millam JM, Iyengar SS, Tomasi J, Barone V, Mennucci B, Cossi M, Scalmani G, Rega N, Petersson GA, Nakatsuji H, Hada M, Ehara M, Toyota K, Fukuda R, Hasegawa J, Ishida M, Nakajima T, Honda Y, Kitao O, Nakai H, Klene M, Li X, Knox JE, Hratchian HP, Cross JB, Adamo C, Jaramillo J, Gomperts R, Stratmann RE, Yazyev O, Austin AJ, Cammi R, Pomelli C, Ochterski JW, Ayala PY, Morokuma K, Voth GA, Salvador P, Dannenberg JJ, Zakrzewski VG, Dapprich S, Daniels AD, Strain MC, Farkas O, Malick DK, Rabuck AD, Raghavachari K, Foresman JB, Ortiz JV, Cui Q, Baboul AG, Clifford S, Cioslowski J, Stefanov BB, Liashenko G Liu, Piskorz AP, Komaromi I, Martin RL, Fox DJ, Keith T, Al-Laham MA, Peng CY, Nanayakkara A, Challacombe M, Gill PMW, Johnson B, Chen W, Wong MW, Gonzalez C, Pople JA (2004) Gaussian, Inc., Wallingford
97. Reed AE, Curtiss LA, Weinhold F (1988) Chem Rev 88:899–926. And references cited therein
98. Bondi A (1964) J Phys Chem 68:441–451
99. Pearson PG (1963) J Am Chem Soc 85:3533–3539
100. Richens DT (1997) The chemistry of aqua ions. Wiley, Chichester
101. Eisler R, Hennekey RJ (1977) Arch Environ Contam Toxicol 6:315–323
102. Lewis DFV, Dobrota M, Taylor MG, Parke DV (1999) Environ Toxicol Chem 18:2199–2204